ADVANCED FUNCTIONAL MATERIALS
www.afm-journal.de

Cation-Alginate Complexes and Their Hydrogels: A Powerful Toolkit for the Development of Next-Generation Sustainable Functional Materials

Pietro Tordi, Francesca Ridi, Paolo Samorì, and Massimo Bonini**

The use of materials from renewable sources instead of fossil fuels is a crucial step forward in the industrial transition toward sustainability. Among polysaccharides, alginate stands out as a versatile and eco-friendly candidate due to its ability to form functional complexes with cations. This review provides an up-to-date and comprehensive description of alginate complexation with specific cations, focusing on how interaction forces can be harnessed to tailor the physicochemical properties of cation-alginate-based functional materials. Methodologies and approaches for the development and multiscale characterization of these materials are introduced and discussed. Alginate complexes with mono-, di-, tri-, and tetravalent cations (namely Ag^{+}, Mg^{2+}, Ca^{2+}, Sr^{2+}, Ba^{2+}, Mn^{2+}, Co^{2+}, Ni^{2+}, Cu^{2+}, Zn^{2+}, Cd^{2+}, Pb^{2+}, UO_2^{2+}, Cr^{3+}, Fe^{3+}, Al^{3+}, Ga^{3+}, Y^{3+}, La^{3+}, Ce^{3+}, Nd^{3+}, Eu^{3+}, Tb^{3+}, Gd^{3+}, Zr^{4+}, Th^{4+}) are reviewed. Each cation is discussed individually, highlighting how it can uniquely influence the material properties thereby unlocking new potentials for the design of advanced functional materials. Key challenges and opportunities in applying these complexes across diverse fields, such as biomedicine, environmental remediation, food additives and supplements, flame retardants, sensors, supercapacitors, catalysis, and mechanical isolators are assessed, providing evidence of the transformative potential of cation-alginate complexes for tackling global challenges and advancing cutting-edge technologies.

1. Introduction

Alginate is an anionic polysaccharide primarily sourced from brown algae of the Phaeophyceae family[1] through alkaline extraction, which was first described by E.C.C Stanford in 1881.[2] However, its presence in certain bacteria has also been documented.[3] Certified as a safe product by the Food and Drug Administration (FDA) and classified as a food additive, alginate finds extensive use in medical, food, and cosmetic applications. The polymer structure, which has been extensively elucidated by means of ^{1}H- and ^{13}C-NMR analyses,[4–7] consists of (1,4) linked β-D-Mannuronate and α-L-Guluronate residues. The ratio of Mannuronate to Guluronate (M/G)[8–10,4] and the sequence of the residues can vary depending on the extraction source, leading to the coexistence within the same polymeric chain of homogeneous (GG or MM) and heterogeneous blocks (GM or MG).[4] Alginates are commercial products typically comprising a G-block content ranging from 14.0% to 31.0%, while their average molecular weight falls between 32 and 400 kDa,[11] resulting in significant differences in the viscosity of aqueous solutions. Another crucial factor affecting the viscosity is the pH level. An increase in proton concentration significantly raises the viscosity, reaching its maximum at pH values close to 3.5. At this pH, carboxylate groups become protonated, promoting strong interchain interactions facilitated by hydrogen bonds.[11] The carboxylate groups existing in the residues can strongly interact at the supramolecular level with cationic species, resulting in the formation of complexes with diverse geometries (see **Figure 1**). This chain reassembling, known as crosslinking, occurs with monovalent, divalent, trivalent, and tetravalent cations, and offers a straightforward method for producing hydrogels. The nature of the complex is heavily influenced by the ion's charge, size, as well as the sequence of the M and G residues, thereby impacting on the properties of the resulting hydrogel. Alginate's biocompatibility and biodegradability, combined with tunable cation interactions, offer a powerful approach to developing advanced materials. This can drive sustainable technologies, improve industrial processes, and reduce reliance on synthetic polymers, promoting eco-friendly

P. Tordi, F. Ridi, M. Bonini
Department of Chemistry "Ugo Schiff" and CSGI
University of Florence
via della Lastruccia 3, Sesto Fiorentino 50019, Florence, Italy
E-mail: massimo.bonini@unifi.it
P. Tordi
University of Strasbourg, CNRS, ISIS UMR 7006
8 Alleé Gaspard Monge, Strasbourg 67000, France
P. Samorì
Institut de Science et d'Ingeniérie Supramoléculaires (ISIS) – Université de Strasbourg and CNRS
8 Alleé Gaspard Monge, Strasbourg F-67000, France
E-mail: samori@unistra.fr

The ORCID identification number(s) for the author(s) of this article can be found under https://doi.org/10.1002/adfm.202416390

DOI: 10.1002/adfm.202416390

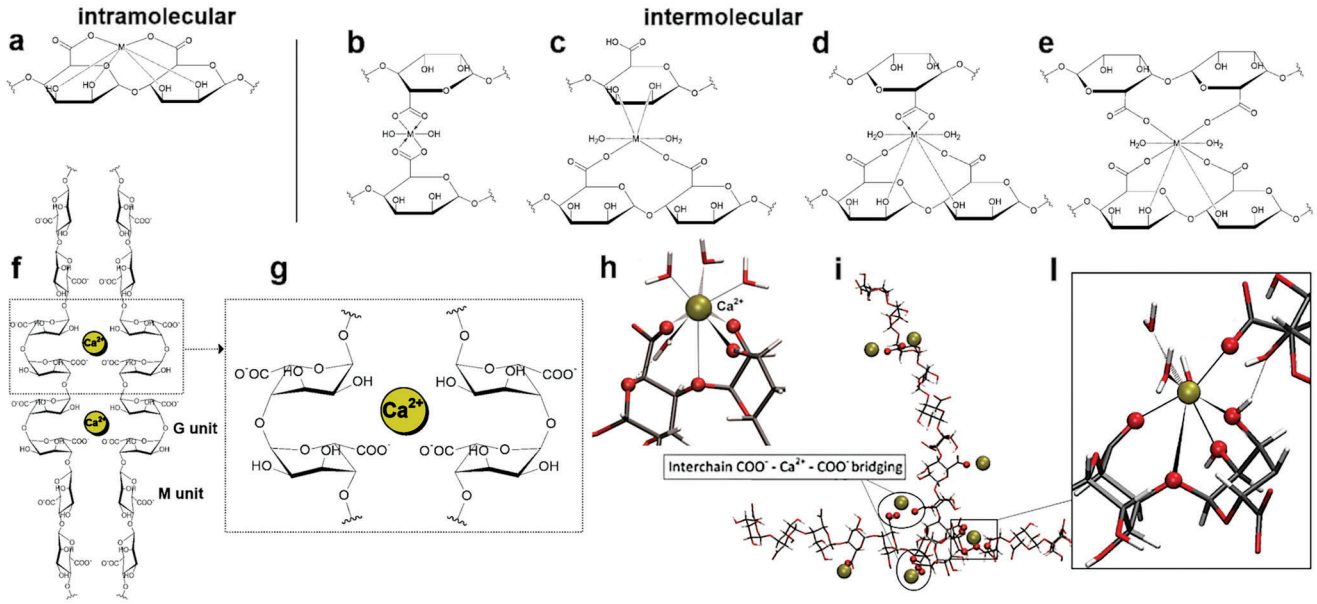

Figure 1. Cation-alginate coordination geometries: intramolecular a) and intermolecular coordination b–e) Adapted with permission.[13] Copyright 1993, John Wiley and Sons. f) Alginate egg box coordination of Ca^{2+} ions, as proposed by Fu et al.,[14] based on Grant's and Morris' evidences.[15,16] Adapted with permission.[17] Copyright 2019, Springer Nature. This panel highlights the role of G units in chelating the Ca^{2+} ions. g) Inset where the coordination geometry is magnified. h) The egg-box binding site for Ca^{2+} and i) two poly-G chains aggregating in a perpendicular motif via three bridging Ca^{2+} ions, as obtained from molecular dynamics simulations. Reproduced with permission.[18] Copyright 2013, Elsevier. The inset highlights the details of the egg box component of this junction zone. Oxygen atoms that are directly interacting with a calcium ion are rendered as small red spheres. In (h) and (i) oxygen atoms on the poly-G chains are shown as red spheres, while coordinated water molecules are shown as stick models.

alternatives for a more sustainable future. Despite extensive research on alginate, to the best of our knowledge only one work has tried to summarize properties and applications of different cation-alginate complexes (limiting the focus to a reduced number of cations):[12] in fact, the extensive literature on alginate poses a challenge in gaining a comprehensive knowledge, discouraging the adoption of a wide perspective and hindering a systematic research in the field.

This review fills a gap in the literature by providing a comprehensive overview of how combining alginate with various cations modulates the physicochemical properties of metal-alginate complexes. Recent studies often focus on individual ions, overlooking broader comparisons across systems. To guide researchers, we have organized the content into distinct sections, highlighting the significant potential of cation-alginate complexes in functional materials development. This structure is designed to engage both novice and expert readers, offering essential knowledge for beginners and a detailed, accessible resource for experienced researchers seeking the latest findings.

Section 2 provides a comprehensive overview of the strategies and characterization techniques crucial for developing cation-alginate complexes and understanding their physical and chemical properties. It covers crosslinking methods, nanocomposite formation, advanced processing, and essential validation techniques. Subsequently, Section 3 explores ion-specific interactions that shape the behavior of these complexes, organized by cation valency to highlight each cation's unique influence on material properties. This detailed analysis, at atomic, molecular, and supramolecular levels, is vital for understanding how cation-alginate complexes can be optimized for designing advanced functional materials. **Table 1** effectively summarizes key aspects of ion-alginate complexation discussed in Section 3, spanning from the molecular level to the properties of the hydrogel matrix.

Finally, in Section 4, the functional applications of these complexes are reviewed, organized by application type to highlight their current uses and future potential. The section emphasizes how interaction strength impacts application suitability (e.g., strong cation interactions enhance toughness and resistance for mechanically demanding uses, while weaker interactions enable cation exchange or release in more dynamic applications). Opportunities and challenges are discussed, proposing a roadmap for future research in this promising field. The information above is summarized in **Table 2**, which highlights the sectors that could benefit from the use of M^{X+}-alginate complexes: the physicochemical properties described in Table 1 impart specific functionalities and, as a consequence, determine the potential for applications.

2. Strategies and Characterization Techniques for the Development of Functional Materials Based on Cation-Alginate Complexes

Cation-alginate complexes are essential for creating functional materials with tunable mechanical properties, biocompatibility, and responsiveness. This section covers key strategies for developing these materials, including crosslinking, composite formation, advanced processing methods, and characterization techniques. We intentionally exclude discussion of chemical modifications to the alginate backbone, as these have been extensively

Table 1. Cation-specific complexation modalities and hydrogel matrix properties. References for each specific ion are also provided.

Cation	Complexation	Hydrogel properties	References
Ag^{+}	- Inter/Intramolecular - Involving carboxylate and hydroxyl groups	- Low-strength gel - Biocompatible - Antimicrobial	[77, 91–94]
Mg^{2+}	- Inter/Intramolecular - Involving carboxylate and hydroxyl groups	- Low-strength gel - Biocompatible	[102–104]
Ca^{2+}	- Inter/Intramolecular - Egg box buckled chain structure involving G blocks	- Medium-strength gel - Biocompatible	[15, 16, 24, 25, 83, 97–99, 101, 108–110, 129]
Sr^{2+}	- Inter/Intramolecular - Egg box buckled chain structure involving G blocks - More interaction sites than Ca^{2+}	- Medium/High-strength gel - Biocompatible - Osteogenic	[32, 97–99, 101, 132, 134–137, 141]
Ba^{2+}	- Inter/intramolecular - Egg box buckled chain structure involving G and M blocks - More stable than Ca^{2+} and Sr^{2+}	- High-strength gel - Biocompatible	[34, 97–99, 101, 142, 143, 145–148]
Mn^{2+}	- Inter/Intramolecular - Involving carboxylate and hydroxyl groups from G and M blocks	- Low/Medium-strength gel - MRI active	[72, 97–99, 101, 153, 156]
Co^{2+}	- Inter/Intramolecular - Involving carboxylate and hydroxyl groups from G and M blocks - Stronger than Mn^{2+}	- Medium-strength gel - Toxic	[72, 97–99, 101, 162]
Ni^{2+}	- Inter/Intramolecular - Involving carboxylate and hydroxyl groups	- Medium-strength gel - Toxic	[97–99, 101, 167, 168, 170, 171]
Cu^{2+}	- Inter/Intramolecular - Egg box buckled chain structure for low Cu^{2+} concentration - Lower binding selectivity than Ca^{2+}	- High-strength gel - Biocompatible - Antimicrobial	[15, 68, 72, 97–99, 101, 175–181]
Zn^{2+}	- Inter/Intramolecular - Involving carboxylate and hydroxyl groups - Not ascribable to egg box	- Medium-strength gel - Biocompatible - Antifouling	[15, 74, 97–99, 101, 189, 190, 196]
Cd^{2+}	- Inter/Intramolecular - Involving carboxylate and hydroxyl groups	- High-strength gel - Toxic	[97–99, 101, 197, 202]
Pb^{2+}	- Inter/Intramolecular - Involving carboxylate and hydroxyl groups	- High-strength gel - Toxic	[97–99, 101, 203–205]
UO_2^{2+}	- Inter/Intramolecular - Involving carboxylate and hydroxyl groups	- Gel strength not documented - Toxic	[208]
Cr^{3+}	- Intermolecular (predominant) - Involving carboxylate and hydroxyl groups	- Gel strength not documented	[209, 211, 212]
Fe^{3+}	- Intermolecular (predominant) - Involving carboxylate and hydroxyl groups - Concurrent alginate protonation	- High-strength gel - Biocompatible	[209, 222–226]
Al^{3+}	- Intermolecular (predominant) - Involving carboxylate and hydroxyl groups - Concurrent alginate protonation	- High-strength gel - Biocompatibility not assessed	[209, 227, 231, 232]
Ga^{3+}	- Intermolecular (predominant) - Involving carboxylate and hydroxyl groups	- Medium-strength gel - Biocompatible - Antimicrobial	[35, 209, 233–236]
Y^{3+}	- Intermolecular (predominant) - Involving carboxylate and hydroxyl groups	- Gel strength not documented - Biocompatibility not assessed	[209, 237–240]
La^{3+}	- Intermolecular (predominant) - Involving carboxylate and hydroxyl groups	- Gel strength not documented - Biocompatibility not assessed	[209, 241, 242, 246]
Ce^{3+}	- Intermolecular (predominant) - Involving carboxylate and hydroxyl groups	- Medium/high-strength gel - Biocompatible - Antimicrobial	[209, 247–250]
Nd^{3+}	- Intermolecular (predominant) - Involving carboxylate and hydroxyl groups	- High-strength gel - Biocompatible - Fluorescent	[75, 209, 251, 252]
Eu^{3+}	- Intermolecular (predominant) - Involving carboxylate and hydroxyl groups	- Gel strength not documented - Fluorescent	[209, 254]

(*Continued*)

Table 1. (Continued)

Cation	Complexation	Hydrogel properties	References
Tb^{3+}	- Intermolecular (predominant) - Involving carboxylate and hydroxyl groups	- Gel strength not documented - Fluorescent	[209, 254]
Gd^{3+}	- Intermolecular (predominant) - Involving carboxylate and hydroxyl groups	- Gel strength not documented - Biocompatible - MRI active	[209, 255]
Zr^{4+}	- Intermolecular - Involving carboxylate and hydroxyl groups - Concurrent alginate protonation	- High-strength gel	[13, 256–260]
Th^{4+}	- Intermolecular - Involving carboxylate and hydroxyl groups	- Gel strength not documented - Toxic	[13, 261, 262]

covered in the literature. Modifications like grafting methacrylate, cyclodextrins, amine groups, oxidation, sulfation, or hydrophobic alterations are well-documented for alginate and other polysaccharides.[19–22]

Readers are encouraged to consult these sources for comprehensive details on such modifications. Within this context, it is important to note that these chemical modifications can significantly enhance the mechanical properties, biocompatibility, and functionality of materials. Additionally, partial chemical modifications can synergistically complement cation-alginate interactions, which are the primary focus of this review.

2.1. Crosslinking Strategies

Crosslinking is a powerful method to form cation-alginate complexes, by transforming the water-soluble polymer into a gel

Table 2. Function and sector of possible impact of the M^{X+}-alginate complexes described in this review. References for each specific cation are also provided.

Function	Sector of possible impact	Cation
Carrier (release and uptake)	– Water purification – Drug delivery – Wound healing – Agriculture	Ag(I)[77,93]; Mg(II)[104]; Ca(II)[24,25,27,108–110,113,115,116]; Ba(II)[149–151]; Mn(II)[160,161]; Ni(II)[69,171,172,174]; Zn(II)[193,196]; Fe(III)[215–218,224–226]; Al(III)[227–230]; Y(III)[238–240]; La(III)[242–244,246]; Ce(III)[249]; Zr(IV)[256–260]
Contrast agent	– Medical imaging	Mn(II)[156–158]; Gd(III)[255]
Scaffold for cell growth	– Tissue engineering – Regenerative medicine	Ca(II)[26,117–120]; Sr(II)[134–141]; Ba(II)[33,145–147]; Mn(II)[157]; Co(II)[165]; Cu(II)[34,179]; Fe(III)[222,223]; Ga(III)[35,236]
Antimicrobial	– Tissue engineering – Wound healing – Antifouling treatments	Cu(II)[177–181]; Zn(II)[74,189,190]; Ga(III)[233,235]; Ce(III)[250]
Food additive and supplements	– Food packaging – Food storage – Dietary supplements – Nutraceuticals	Ca(II)[29,30,128–131]; Zn(II)[31]
Flame retardant	– Automotive – Textiles – Building and construction – Wires and cables – Electronics	Ba(II)[144]; Mn(II)[81]; Co(II)[81,166]; Ni(II)[169]; Zn(II)[80,192]; Fe(III)[79]; Al(III)[79,231]
Catalyst	– Organic synthesis – Water purification	Cu(II)[182–184]
Supercapacitor[263]	– Automotive – Electronic devices – e-skins	Ca(II)[122]; Zn(II)[194]
Sensor	– Environmental monitoring – Physiological monitoring – Robotics – e-skins	Ca(II)[125–127]; Mn(II)[76]; Cu(II)[76,185]; Fe(III)[76]; Eu(III)[254]; Tb(III)[254]; Zr(IV)[76]
Vibration isolator	– Automotive – Aerospace – Construction – Electronics	Al(III)[232]

or solid material with specific mechanical and structural properties. The choice of cation and crosslinking method dramatically affects the properties of the final material, as highlighted in the following section where cations are individually discussed. The most commonly employed method involves the ionic crosslinking of alginate with divalent cations like calcium (Ca^{2+}).[23–27] This process leads to the formation of hydrogels through interactions between the cations and the G-blocks of alginate. Calcium-alginate gels are widely used due to their biocompatibility and ease of gelation, making them ideal materials for agriculture,[28] food,[29–31] and biomedical applications,[32–35] such as soil conditioners, controlled-release fertilizers, gelling agents, edible films, wound dressings, and drug delivery systems.

Crosslinked alginate networks can be formed through either external or internal gelation. In external gelation, the crosslinker diffuses toward the interior of the polymer solution. In internal gelation, the crosslinker is embedded within the alginate in an insoluble form and is gradually released (typically by lowering the pH of the medium), often by adding a reactant. Controlling the crosslinking kinetics allows for the preparation of networks with different mechanical strengths and stabilities, as well as materials with anisotropic properties. Layered crosslinking is also possible, adopting an external gelation approach[25]: this advanced technique often involves the sequential layering of different cations, which can create materials with gradient properties or hierarchical structures. Layered crosslinking can also be achieved using a single cation as a function of its concentration. The diffusion process creates uneven concentration gradients of the crosslinker, leading to discontinuities in the gel's physicochemical properties. This method is useful for developing materials with complex mechanical requirements, such as those required for the successful integration into multifunctional biomedical devices.

2.2. Composites

Cation-alginate complexes can function as matrices that allow for the incorporation of specific micro- and/or nanomaterials to enhance the properties of the composite. This can be done either by using cations as precursors for the in situ formation of nanostructures or by adding pre-formed nano- or microstructures to alginate dispersions, where they can act as active crosslinkers or fillers. This approach improves the material's functionality, introducing additional properties, such as conductivity, magnetism, or antimicrobial activity, depending on the specific materials utilized.[36–39]

Embedding metallic nanoparticles (NPs) like silver or gold into cation-alginate matrices can impart antimicrobial[40–42] and/or catalytic properties[43,44] to the material. For example, silver nanoparticle-enhanced calcium-alginate hydrogels have demonstrated significant promise in wound healing applications by preventing bacterial infections and promoting tissue regeneration.[45,46]

The combination of magnetic nanoparticles with cation-alginate complexes allows for the design of magnetically responsive materials, which are highly valuable in targeted drug delivery,[47] where an external magnetic field can direct the material to a specific location in the body, or in environmental cleanup efforts,[48] where magnetic fields can be used to recover the material after it has adsorbed pollutants.

By incorporating conductive nanomaterials, such as graphene, carbon nanotubes, or 2D metal carbides (MXenes) into cation-alginate complexes, electrically active hydrogels or films can be fabricated.[49–54] These materials are ideal for flexible electronics, electromagnetic shielding, biosensors, and electroactive tissue engineering, where electrical stimulation impacts cell behavior and tissue growth.

Graphene and MXenes have also been shown as effective fillers in nanocomposites including alginate for the preparation of ion-selective membranes for different applications, such as enhanced ion-sieving membranes for recovery of acids from iron-containing wastewater[55] and for osmotic energy harvesting by reverse electrodialysis.[56]

SiO_2 reinforced-alginate hybrid films have been shown to improve the poor Coulombic efficiency and unsatisfactory lifespan of aqueous rechargeable Zn metal batteries[57]; in fact, the ability to modulate metal solid–liquid interaction energy and spatial distribution of all species in the electric double layer (EDL) near the Zn electrode stabilizes the Zn/electrolyte interface which often causes Zn dendrite growth and side reactions.

2.3. Advanced Processing Techniques

Processing techniques are crucial in shaping cation-alginate complexes into functional forms that meet specific application needs. The method of processing often dictates the material's morphology, mechanical properties, and overall performance. As mentioned earlier, the ability to control the kinetics of cation crosslinking allows for the creation of complex, gradient materials with customized mechanical and biological properties. This can be best achieved through a subtle control over the interplay of concentration (of both cation and alginate), viscosity, and processing technique, such as casting, extrusion, spraying, etc.[58–60]

Cation-alginate complexes and hydrogels are highly compatible with 2D and 3D printing technologies, which allow for the high-throughput fabrication of intricate, custom-shaped structures. These methods are particularly beneficial in creating patient-specific implants or scaffolds for tissue engineering,[58] where precise geometry, tunable porosity, and structural integrity are critical, as well as microparticles for the immobilization and culture of algal cells and single cell encapsulations.[17]

Highly porous, low-density structures with controlled pore size and distribution can be prepared by freeze-drying cation-alginate gels.[61] These materials are ideal for use in tissue engineering, where porosity is necessary for cell infiltration and nutrient diffusion, an in environmental applications, where high surface area is crucial for adsorption processes.

Another strategy toward the preparation of materials with high surface area and tunable porosity is electrospinning,[62] which can be used to produce nanofibrous mats of cation-alginate complexes. These characteristics are advantageous for applications such as tissue scaffolds, where the high surface area promotes cell attachment and growth, or in filtration membranes, where porosity is key to performance.

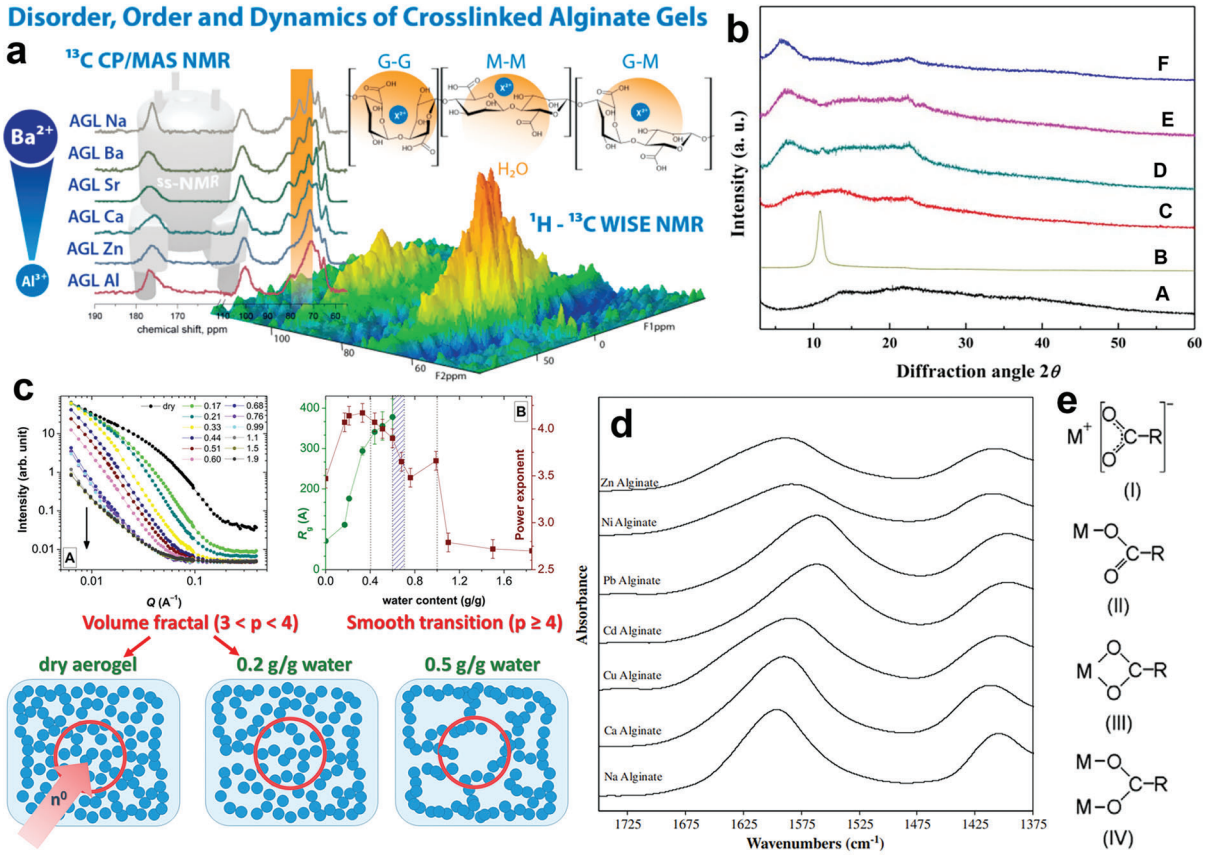

Figure 2. a) Sketch illustrating the potential of NMR in studying M^{X+}-crosslinked alginate samples. Adapted with permission.[63] Copyright 2017, American Chemical Society. b) XRD patterns of (A) Na-alg, (B) GO (graphene oxide), (C) Na-alg/GO, (D) Ca-alg/GO, (E) Ba-alg/GO, and (F) Fe-alg/GO. Adapted with permission.[65] Copyright 2016, John Wiley and Sons. c) Small-angle neutron scattering (SANS) measurements of Ca-alginate aerogel (CaAG) at various hydration levels (A). The scattering curves represent CaAG samples with different water contents, and have been vertically offset for clarity. The arrow indicates the direction of increasing water content in the samples, with the specific water contents provided in the legend in g/g units. Power exponent (p) values and gyration radius, estimated using the Beaucage model, plotted as a function of the water content in CaAG. The dotted vertical lines mark the approximate water content levels at which notable structural changes take place (B). Adapted with permission.[66] Copyright 2021, American Chemical Society. d) FT-IR spectra of (from bottom to top) $Na^+/Ca^{2+}/Cu^{2+}/Cd^{2+}/Pb^{2+}/Ni^{2+}/Zn^{2+}$-crosslinked alginate and e) coordination geometries for the M^{X+}-carboxylate coordination: ionic (I), monodentate (II), bidentate chelating (III), and bidentate bridging (IV). Adapted with permission.[64] Copyright 2009, Elsevier.

2.4. Characterization Techniques for Validating Cation-Alginate Complexes

Developing functional materials based on cation-alginate complexes requires thorough, multiscale characterization to link structure and properties, ensuring they meet application-specific requirements. This section offers a guide to key characterization tools relevant for designing and optimizing these materials. Techniques are organized by the specific properties they assess, enabling a more efficient, targeted approach. By utilizing these comprehensive methods, researchers can rigorously validate the properties and functionalities of cation-alginate complexes, ensuring their suitability for various practical applications.

2.4.1. Structural and Compositional Analysis

To unravel the structural and compositional characteristics of these complexes, several techniques could be employed. Nuclear magnetic resonance (NMR) spectroscopy is a powerful tool for unraveling the assembly of the alginate chains around the cationic species, reaching atomic-resolution (see **Figure 2**).[63] Fourier transform infrared spectroscopy (FT-IR) is instrumental in confirming interactions between alginate and cations, as it identifies shifts in characteristic absorption bands.[64] This method is particularly useful for revealing the extent of crosslinking and the presence of specific functional groups within the complex. X-ray diffraction (XRD)[65] further complements this by providing insights into the crystalline structure, especially when filler materials are incorporated. Through XRD, the phase distribution and crystallinity, which are critical for assessing the material's mechanical properties and overall stability, can be assessed. Small angle scattering of neutrons and X-rays (SANS and SAXS)[66–68] can significantly complement structural studies by providing detailed insights into the nanostructure of cation-alginate complexes, with the distinct advantage of allowing the investigation of hydrated samples, such as hydrogels, in their native state without the

need for drying, thereby preserving their inherent structural characteristics.

For compositional analysis, inductively coupled plasma atomic emission spectroscopy (ICP-AES) is used to precisely quantify the elements in the cation-alginate complexes. This technique is particularly valuable for determining the concentration and distribution of cations within the material, providing essential data for understanding how these ions influence the material's properties. When focusing on the surface elemental composition and chemical states, X-ray photoelectron spectroscopy (XPS) plays a crucial role, thereby confirming the presence of cations and understanding the nature of their binding with the alginate.[69]

2.4.2. Morphological and Microstructural Analysis

Examining the morphology and microstructure of cation-alginate complexes requires the use of advanced imaging techniques, especially in composites where fillers are incorporated within alginate. Field emission scanning electron microscopy (FE-SEM)[25] offers high-resolution images of the surface without the need for metallization, allowing for detailed observation of porosity, surface roughness, and, when present, the distribution of filler particles. For an even more detailed view of the internal nanostructure, transmission electron microscopy (TEM) could be employed. TEM provides essential information on the dispersion, size, and interaction of fillers within the alginate matrix, which is vital for understanding how composites will perform in various applications. Additionally, Cryo-transmission electron microscopy (cryo-TEM) can be utilized to examine thin sections of hydrogels at cryogenic temperatures, preserving their native hydrated state and providing further insights into their internal structure and interactions without the need for drying. Atomic force microscopy (AFM) and confocal laser scanning microscopy (CLSM) are effective in analyzing the interior morphology of cation-alginate hydrogels,[70,71] where uniform crosslinking plays a critical role. This uniformity not only ensures the long-term stability of the microcapsules but also significantly influences their mechanical properties, such as elasticity and resistance to deformation.

2.4.3. Mechanical Properties

Understanding the mechanical properties of cation-alginate complexes is crucial, particularly for applications requiring robust materials. Rheometry is commonly exploited to assess the viscoelastic properties of hydrogels.[14,23,72] By examining gelation kinetics and crosslinking density, rheometry offers detailed information on the mechanical stability of the materials under stress. Furthermore, the results from rheometry can be analyzed using various models to derive structural insight on the network, which helps in understanding the material's behavior under different conditions.

Tensile and compression testing are essential for evaluating the mechanical strength, elasticity, and durability of the complexes.[73–75] These tests are particularly important for applications like load-bearing tissue scaffolds, where mechanical performance is critical. As the development of functional materials expands into areas, such as wound healing patches, sensors, and artificial skins, adhesion tests are becoming increasingly relevant, especially to evaluate the ability of the materials to adhere to different surfaces, which is crucial for ensuring effective performance in practical applications.

2.4.4. Thermal Properties

The thermal behavior of cation-alginate complexes is another key area of focus. Differential scanning calorimetry (DSC) is utilized to investigate thermal transitions, such as the glass transition temperature (T_g), which can indicate changes in the self-assembly dictated by cation interactions.[76,77] Additionally, low-temperature differential scanning calorimetry (LT-DSC) is particularly relevant for understanding the interaction between cation-alginate complexes and water.[78] In fact, LT-DSC allows for the quantification of free and bound water within the material, offering valuable insights into how water influences the thermal properties and stability of the complexes. This technique provides essential information on the hydration state of the material, which is crucial for applications involving moisture-sensitive environments.

Thermogravimetric analysis (TGA) is also critical, as it monitors weight loss with temperature, providing important insights into the thermal degradation behavior of the material (which often depends on the presence of different cations) and the content of any incorporated solid material.[79–81]

2.4.5. Swelling and Degradation Behavior

Swelling and degradation behaviors are important for applications like soil conditioning, edible films, drug delivery, and tissue engineering.[82,83] Swelling ratio measurements provide information on the crosslinking density and the material's responsiveness to environmental conditions. These measurements are crucial for designing materials that can perform effectively in specific settings. Notably, in vitro degradation tests are conducted to monitor the rate of degradation under physiological conditions,[83,84] helping to predict the material's lifespan and performance in biomedical contexts. These tests also offer insights into how different cations affect the stability and durability of the material. In particular, swelling and degradation tests serve as important prescreening tools to assess the suitability of samples before more complex and costly biological tests are carried out, ensuring that only the most promising candidates advance to the next stage of evaluation.

2.4.6. Biological Properties

Finally, the biological properties of cation-alginate complexes are of paramount importance, especially for biomedical applications. Ensuring biocompatibility is a critical step, and this is often achieved through cytotoxicity assays, such as MTT or Live/Dead staining.[85–87] These assays evaluate the impact of the complexes on cell viability, which is essential for ensuring their safety and effectiveness in medical contexts. Additionally, cell adhesion and proliferation studies are conducted to assess how well cells adhere to and proliferate on cation-alginate scaffolds. The data are

crucial for applications in tissue engineering and regenerative medicine, where the interaction between the material and biological cells is a key factor in success.

3. Ion-Specific Interactions and Their Impact on Cation-Alginate Complexes

The previous section's strategies and validation techniques highlight the versatility of cation-alginate complexes in material design. Their tunability, biocompatibility, and sustainability make them a key platform for next-generation materials. This section delves into the interactions between alginate and various cations, grouped by valence. The cation's nature crucially impacts properties like gelation behavior, mechanical strength, and thermal stability. By examining monovalent, divalent, trivalent, and tetravalent cations, we offer a comprehensive overview of how these interactions shape functional materials, enabling customization for specific applications.

3.1. Monovalent Cations

Alginate is notorious for its strong affinity toward divalent cations, such as calcium and strontium, also because of the relevance of these cations in biomedical[11] and food applications.[88] However, this focus often overlooks instances where alginate also coordinates monovalent cations like sodium, potassium, and, more relevant toward functional materials, silver.

3.1.1. Silver

Despite the widespread use of alginate composite materials containing silver nanoparticles or silver flakes,[42,89] there is a scarcity of literature offering a molecular level insight into the crosslinking of alginate with silver cations. This shortage can be attributed to the relatively weak nature of the Ag^+-alginate interaction, often ascribed to the large ionic radius of Ag^+ (1.15 Å),[90] which limits the number of accessible binding sites and the diversity of products that can be obtained. Nevertheless, the antimicrobial, electronic, and SERS (surface-enhanced Raman spectroscopy)-enhancing properties of Ag have garnered significant interest from researchers. Hassan and co-workers performed FT-IR spectroscopy studies on silver-alginate complexes, and concluded that in analogy to divalent cations, the Ag^+-binding could occur either at the intermolecular or at the intramolecular level (see Figure 1a).[91] At the intermolecular level alginate has the ability to interact with one Ag^+ ion by means of either two carboxylate groups or one carboxylate and one hydroxyl group from separate alginate chains, resulting in the formation of a planar complex perpendicular to the plane of the polymeric chains. At the intramolecular level, silver can coordinate the carboxylate groups belonging to two neighboring glycosidic units.[91] Moreover, the conductivity of Ag^+-alginate hydrogels suggests that the coordination of silver can induce the decarboxylation of alginate, eventually resulting in the reduction of Ag^+ ions.[91,92] Hollow Ag^+-alginate microcontainers, designed for precise drug release targeting and responsive to ultrasounds, were developed by Lengert et al.[93] The Ag^+-alginate backbone is prepared initially, followed by treatment with ascorbic acid, resulting in a homogeneous distribution of AgNPs (silver nanoparticles) throughout the device. The presence of silver not only guarantees device biocompatibility but also enhances Raman signals, encouraging future application in theranostics.[93] However, the weak interaction between alginate and Ag^+ makes it challenging to produce hydrogels with complex shapes, such as fibers, which significantly limits the potential applications of Ag^+-alginate complexes.[94,95] On this topic, we have recently demonstrated that Ag^+-crosslinked alginate can be obtained through wet spinning: the optimization of multiple boundary conditions (such as the flow of extrusion and the concentrations of both the polymeric solution and the crosslinking bath) made it possible to obtain fibers with lengths up to several meters with consistent cross-sections.[77] The Ag^+ ions can be easily reduced using mixtures of citric and ascorbic acid, to decorate the surface with homogeneously distributed AgNPs.[77]

3.2. Divalent Cations

Divalent cations represent the largest subset of ions interacting with alginate to form crosslinked structures. The following M^{2+} ions are reportedly capable of crosslinking alginate: Mg^{2+}, Ca^{2+}, Sr^{2+}, Ba^{2+}, Mn^{2+}, Co^{2+}, Ni^{2+}, Cu^{2+}, Zn^{2+}, Cd^{2+}, Pb^{2+}, UO_2^{2+}. The crosslinking of the polymeric chains can occur by forming inter or intramolecular complexes.[13] Brus et al. demonstrated through NMR studies that these structures can vary to some extent depending on the type of ion, exhibiting decreased regularity with the decreasing ionic radius (see Figure 2).[63] FT-IR spectroscopy was used by Papageorgiou et al. to determine the coordination geometries between cations and carboxylate groups on the alginate backbone (see Figure 2).[64] Such an assessment relies on the consideration of the carboxylate groups asymmetric and symmetric stretching (ν) vibrations and derives from Nakamoto's work on cation-carboxylate complexes.[96] The addition of divalent cations to sodium alginate solutions can determine change in pH, which affects the affinity between alginate and M^{2+} ions. The systematic work by Haug et al. and Seely et al., involving pH evaluation and complexometric titration, respectively, made it possible to order most of the divalent ions previously introduced in terms of their affinity toward alginate:[97–99] $Pb^{2+} > Cu^{2+} > Cd^{2+} > Ba^{2+} > Sr^{2+} > Ca^{2+} > Co^{2+} \approx Ni^{2+} \approx Zn^{2+} > Mn^{2+}$. Schweiger et al. demonstrated by viscometric analysis that the stability of the M^{2+}-alginate complex, among alkaline-earth metals, decreases upon lowering the ion size.[100] Increasing the amount of EDTA in solutions containing crosslinked polymeric chains produces an increase in the viscosity due to the sequestration of cations by EDTA and to the increase of the interaction between alginate chains and water. The cation is the main factor regulating this effect: a higher EDTA concentration is required in high-stability cation-alginate complexes to reach maximum viscosity when compared to low-stability ones.[100] The Young modulus of M^{2+}-alginate hydrogels follows the following trend: $Cd^{2+} > Ba^{2+} > Cu^{2+} > Ca^{2+} > Ni^{2+} > Co^{2+} > Mn^{2+}$.[101] It is clear that the macroscopic properties of alginate gels not always align with the previously reported affinity scale. The latter, however, remains a

useful tool to rationalize multiple phenomena. All the aforementioned M^{2+} cations will be detailed in the following paragraphs.

3.2.1. Magnesium

Mg^{2+} is the least investigated among the divalent cations, most reasonably due to its small size, which lowers the stability of its complexes with alginate. The crosslinking phenomenon, however, could be relevant to many applications, such as in the case of water filtration systems, where it can induce polysaccharide fouling in membranes.[102]

Topuz et al. conducted rheological studies on the gel formation process occurring between alginate and magnesium, emphasizing its slow kinetics, which is dependent on the concentration of both inorganic and organic components.[103] Additionally they noticed that an increased number of G units enhances the strength of the resulting gels: however, the crosslinked structures exhibited low stability in water.[103]

An intriguing and promising perspective is the use of Mg^{2+}-alginate formulations to treat gastroesophageal reflux in infants, suggested for the first time by Baldassarre et al.[104] In this framework, the reduced stability of the complexes represents a potential advantage toward the exchange with more effective ions.

3.2.2. Calcium

Among the divalent cations interacting with alginate, calcium is undoubtedly the most extensively studied, owing to both the strength of its interactions and its significance in biomedical applications. Although it is capable of binding both the mannuronate and guluronate residues on alginate, Ca^{2+} is believed to form "egg box" junctions (ionically interacting with $-COO^-$ groups) only with poly-guluronate sequences (see Figure 1f,g).[83] In this case, the binding strength is superior with respect to mannuronate complexes, resulting in the formation of gels that are kinetically stable against dissociation.[83,105,106] The term "egg box" was used for the first time by Grant to describe the geometry of interaction between alginate chains and Ca^{2+} ions.[15] Circular dichroism (CD) combined with computer modeling provided evidence for the formation of this buckled chain structure (see Figure 1h) which takes place through cooperative organization of the functional groups on the alginate backbone crosslinking Ca^{2+} ions.[15,16]

Small angle X-ray scattering was found to be a powerful technique to shed light on Ca^{2+}-alginate interaction, suggesting that the homoguluronic acid sequences associate laterally during the complexation.[67] Interestingly, authors concluded that alginate's mannuronic acid residues act as elasticity moderators (increasing the flexibility of the crosslinked chains), while guluronic acid units produce crosslinked regions with high rigidity,[107] acting similarly to a block copolymer.

Farrés et al. highlighted, through rheological analysis, that high weight averaged molecular weight (M_w) alginates form Ca^{2+}-alginate gels faster compared to their lower M_w counterparts (with equivalent M/G).[23] The measurements were performed while gradually releasing Ca^{2+} ions from $CaCO_3$ using GDL (glucono-δ-lactone) and maintaining a neutral pH. This approach allowed the authors to isolate the effect of the cation on the polymer assembly, separating it from the effects of its concentration and pH.

Ca^{2+}-alginate gels are suitable for use as carriers in drug delivery and food supplement systems, owing to their easily modifiable properties and biocompatibility. To this purpose, alginate-based food supplements are often prepared in the form of beads, commonly dropping an alginate solution in a Ca^{2+}-containing crosslinking bath.[108–110] Multiple preparation parameters (e.g., concentration of alginate and Ca^{2+} solutions and the crosslinking time) can be adjusted to obtain specific release kinetics.[111] Alternatively, Poncelet et al. prepared Ca^{2+}-alginate beads via internal ionotropic gelation in emulsion, dispersing calcium carbonate (almost insoluble in water at neutral pH[112]) in an alginate solution and inducing its gradual dissolution through acidification.[113]

The diffusion of BSA (bovine serum albumin) in Ca^{2+}-alginate hydrogels was found to be susceptible to the guluronate content. In fact, it was shown that an increasing amount of G blocks lowers the diffusion kinetics, as a consequence of the higher rigidity of the crosslinked structure obtained.[24] Voo et al. developed ultrahigh concentration (UHC) Ca^{2+}-alginate beads capable of prolonging methylene blue release 2.5 times longer than normal Ca^{2+}-alginate beads.[25] The study also highlighted that a high Ca^{2+} ions concentration in the crosslinking bath induces a stratified structure in the obtained Ca^{2+}-alginate beads. The fast crosslinking and water expulsion processes were suggested to be responsible for the phenomenon, as schematically represented in **Figure 3**.

Interestingly, micrometer-sized Ca^{2+}-alginate beads can mimic the mechanical properties of human cells: in this case the required monodispersity can be easily reached through microfluidics.[114]

The water purification sector can benefit from Ca^{2+}-alginate matrices, especially the removal of metal ions through ion exchange: Cu^{2+}, Cd^{2+}, and Pb^{2+} are reportedly absorbed by Ca^{2+}-alginate beads.[115] In this context, Tao et al. developed nanostructured crosslinked Ca^{2+}-alginate hydrogels characterized by fast adsorption kinetics for Cu^{2+} and Cd^{2+} at room temperature,[116] while Papageorgiou's Ca^{2+}-alginate beads proved to be selective toward Pb^{2+} ions.[27]

In tissue engineering, the flexibility and biocompatibility of Ca^{2+}-crosslinked alginate matrices are advantageous. Tubular scaffolds with controlled diameter and good cell viability can be easily prepared through electrodeposition, serving as excellent candidates to realize cell-oriented scaffolds.[26] Chondrocytes-loaded Ca^{2+}-alginate scaffolds with good cell viability were employed by Paige et al., to generate cartilaginous tissue de novo in mice.[117] Weber et al. also demonstrated that Ca^{2+}-alginate hydrogels can be used to repair tympanic membrane perforations in Chinchilla,[118] while injectable formulations of that type are suitable for endovascular embolization purposes.[119]

It is worth mentioning that the strong interaction between alginate and Ca^{2+} ions allows for the preparation of alginate hydrogels with filiform structures, adopting a wet spinning approach.[120,121] These products show high tensile strength and a low cytotoxicity, being suitable for wound healing applications.[120]

Superstiff Ca^{2+}-alginate supercapacitors were developed by Ji et al.: the polymeric matrix was used as a sponge, loading

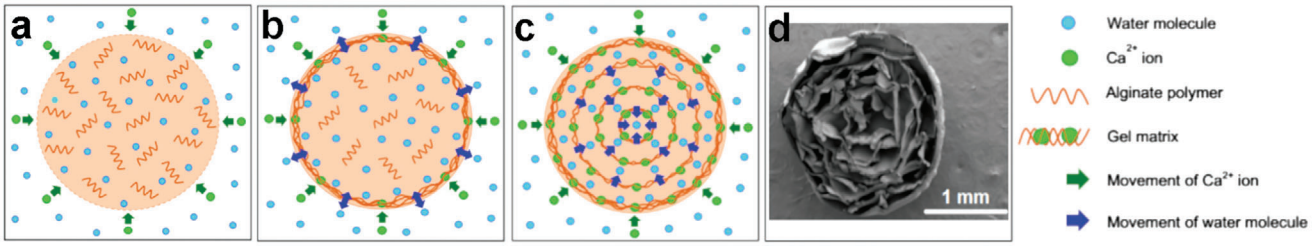

Figure 3. Hypothesized mechanism (a, b, and c are sequential) of Ca^{2+}-alginate gel formation in ultra-high concentration (UHC) alginate beads (from 10% w/v alginate solution).[25] d) Cross-sectional scanning electron microscope image of an UHC alginate bead, highlighting its layered structure. Adapted with permission.[25] Copyright 2016, Elsevier.

huge amounts of Li^{+} and Fe^{3+} (the latter acting as additional crosslinker) to increase both the ionic conductivity and the capacitance.[122] In this framework, it is useful to point out that dried Ca^{2+}-crosslinked alginate starts to degrade around 200 °C (decarboxylation), showing therefore lower thermal stability compared to sodium alginate.[123,124]

Guo et al. developed Ca^{2+}-crosslinked/polyacrylamide alginate fibers, suitable as optical fibers: their flexibility, biocompatibility, and stretchability make these fibers promising building blocks for wearable sensors.[125] Regarding this topic, calcium-alginate hydrogel structures were profitably used as strain sensors taking advantage of their good ionic conductivity and significant flexibility.[126,127]

The food industry can take advantage of Ca^{2+}-alginate formulations in multiple fields. For instance, Ca^{2+}-alginate emulsion gels have been proposed as additives for the preparation of low-fat mayonnaise.[128] Furthermore Ca^{2+}-alginate microbeads obtained by emulsification have been suggested for *Spirulina* (a health beneficial alga) encapsulation, to enhance the taste and nutritional content of yogurt.[129] Ca^{2+}-alginate edible coatings loaded with essential oils have demonstrated the ability to improve the postharvest quality of raspberries,[29] while the use of natamycin-loaded Ca^{2+}-alginate films was suggested for antimicrobial food packaging.[130] Moreover, Vitamin B12 encapsulation and controlled release can be easily achieved using Ca^{2+}-alginate-PVA(polyvinyl acetate) scaffolds.[30] Deng et al. reported the preparation of Ca^{2+}-alginate microbeads with immobilized polygalacturonase enzyme for apple juice clarification.[131]

3.2.3. Strontium

Strontium is characterized by strong affinity toward alginate, which, along with its osteogenic properties, is the primary reason for its application potential. Zhang et al. demonstrated by means of mechanical and FT-IR investigations on alginate fibers that the Sr^{2+}-alginate interaction is stronger than the Ca^{2+}-alginate one, probably due to the presence of a higher number of interaction sites.[32] This finding is supported by the Agulhon's DFT (Density Functional Theory) calculations performed on some alginate complexes with transition/alkaline earth divalent cations.[132]

Crosslinking alginate with Sr^{2+} ions is a viable method to prepare functional hydrogels with huge application potential. Rheological analysis performed by Pastore et al. revealed that Sr^{2+}-alginate gels experience two regimes of stress relaxation.[133] The first, on early/intermediate length scales, can be ascribed to local relaxations (break of physical crosslinking junctions). The second, at a longer time, suggests the occurrence of a more collective rearrangement, such as syneresis and aging.[133] It is interesting to note that hitherto no studies focusing on the thermal properties of Sr^{2+}-alginate gels have been reported.

The known osteogenic properties of strontium push the research activity on Sr^{2+}-alginate hydrogels. Scaffolds were prepared by adding a Sr^{2+}-containing aqueous solution to an alginate-containing one, possibly incorporating additional elements, such as collagen.[134–136] Yuan et al. also investigated the use of Sr^{2+}-alginate coordination to prepare coatings for titanium surfaces: Sr^{2+} release proved to be long-lasting and capable of increasing osteoblast-like cell (MG63) proliferation.[137]

Injectable Sr^{2+}-alginate hydrogel formulations, with or without hydroxyapatite (HAP) and tricalcium phosphate (TCP) as fillers, are reportedly osteogenic.[138–140] Concerning this topic, Neves et al. developed an injectable Sr^{2+}-alginate soft hydrogel containing Sr^{2+}crosslinked alginate beads to obtain a composite with tunable Sr^{2+} release kinetics.[141]

3.2.4. Barium

Ba^{2+}-alginate complexes are the most stable among the alkaline-earth derivatives, due to Ba^{2+} capability of crosslinking both guluronate and mannuronate functionalities of the polymeric backbone.[142,143] This high affinity toward alginate leads to a fast crosslinking that reduces the homogeneity of Ba^{2+}-alginate hydrogels with respect to the Ca^{2+}-crosslinked ones.[142] Thermogravimetric analysis (TGA) showed that dry Ba^{2+}-alginate gels undergo decarboxylation around 205 °C, analogously to Ca^{2+}-alginate ones. Moreover, the high residue in the 300–500 °C interval (significantly superior to that of sodium alginate) clearly indicated that Ba^{2+}-crosslinked alginate can find application as flame retardant.[144]

These networks were proven to be an excellent matrix for cell encapsulation: the low permeability toward antibodies reduces inflammatory reactions when used in allo- and xeno-graft transplantation,[33,145,146] without introducing permselective layers, such as poly-L-lysine (PLL) or poly-ethylene-glycol onto the surface.[147] Transplantation experiments conducted by Zekhorn et al., with Ba^{2+}-alginate encapsulated rat islets, revealed a significant prolongation of postprandial normoglycaemia in recipient mice for at least several weeks, while nonencapsulated islets induced normoglycemia for only a few days.[148] Ba^{2+}-alginate beads also demonstrated a higher affinity for chromium (VI)

with respect to Ca^{2+}-alginate ones, resulting capable of physically adsorbing significant amounts of the aforementioned chemical species.[149] Concerning chemicals removal, Xu et al. proposed Ba^{2+}-alginate beads as a novel adsorbent for sulfate removal in lithium refining.[150] Zhang et al. realized a Ba^{2+}-alginate-PET(polyethylene terephthalate) composite membrane capable of performing molecule/ion separation.[151] Methylene blue (MB) was found to be selectively separated from NaCl (99.5% rejection of MB and 8.3% rejection of NaCl) more efficiently than in analogous devices based on Ca^{2+}-crosslinked alginate.[151]

The good stability of the Ba^{2+}-alginate hydrogel structure in the swollen state—reported in the aforementioned works—was shown to be particularly promising for water purification purposes.[152]

3.2.5. Manganese

Although the interaction between Mn^{2+} and alginate is one of the weakest reported in the literature, Mn^{2+}-alginate complexes possess unique properties: the five unpaired electrons in Mn^{2+} valence shell (and the consequent paramagnetic character) make Mn^{2+}-alginate hydrogels particularly intriguing for applications related to magnetic resonance spectroscopy and imaging (MRI).

Paramagnetic-induced peak broadening allows the study of the interaction between alginate and manganese divalent cations through ^{13}C-NMR. In this way, Emmerichs et al. highlighted that poly-mannuronate alginate sections, due to their stretched ribbon-like structures, interact with C-6 and C-5 carbons. On the other hand, poly-guluronate moieties interact with Mn^{2+} ions through C-6, C-5, and C-1 carbons, forming structures with higher integration of the cation.[153]

Agulhon et al. investigated the rheological properties of Mn^{2+}-alginate formulations revealing that storage and loss modulus (G' and G'', respectively) always intersect, regardless of the guluronate content of the alginate[72]: therefore, such system cannot be defined as gel according to the old IUPAC classification,[154] although the term can be used according to the recent IUPAC terminology.[155] TGA analysis showed that crosslinking sodium alginate with Mn^{2+} ions lowers the decarboxylation onset (around 200 °C) with respect to sodium alginate.[81] However, the low amount of gaseous products released upon heating makes Mn^{2+}-alginate gels intriguing as flame retardants.[81]

Mn^{2+}-alginate hydrogels were profitably used as a system for controlled release of Mn^{2+} ions for applications in manganese-enhanced MRI (MEMRI)[156] and proved to be biocompatible and unable to generate immune response when implanted.[157] Using a microfluidic approach, Su et al. also developed doxorubicin-loaded Mn^{2+}-crosslinked alginate nanoparticles for cancer therapy.[158] In this system, doxorubicin acted as chemotherapeutics generating a large amount of H_2O_2 in the proximity of tumor cells, while Mn^{2+}enhanced MRI contrast and acted as chemodynamic therapeutic generating hydroxyl radicals through a Fenton-like reaction.[158,159]

Interestingly, Mn^{2+}-crosslinked alginate/gelatin organohydrogels (MnAlgGel) demonstrated photoresponsivity under visible light (see **Figure 4**)[76]: the MnAlgGel matrix, due to its higher tendency trap electrons, shows photocurrent (9.2 μA W^{-1}) and photoswitching speed (2.23/3.13 s) superior to that of Cu^{2+}- Fe^{3+}- and Zr^{4+}-crosslinked analogues. This family of gels is also sensitive to temperature, humidity, and strain with excellent cyclability.[76]

Finally, Mn^{2+}-crosslinked alginate is a good candidate for the removal of arsenite (III), arsenate (V), cadmium (II), and chromium (VI) ions in water.[160,161]

3.2.6. Cobalt

Co^{2+}-alginate gels have garnered limited attention compared to those of other divalent cations, mostly due the toxicity associated with this element.[162] Nevertheless, its affinity for alginate and the appropriate dosage have demonstrated significant potential for specific applications.

Rheological studies revealed that for Co^{2+}-alginate gels with low guluronate content, the storage (G') and loss (G'') moduli intersected at higher angular frequency with respect to their Mn^{2+} equivalents.[72] Additionally, high guluronate-content Co^{2+}-alginate gels did not exhibit a crossover point ($G' = G''$), unlike the Mn^{2+}-alginate equivalents. This suggests a stronger interaction between Co^{2+} ions and alginate chains, in agreement with the affinity scale previously reported.

Co^{2+}-alginate gels were used as green, low-cost precursors for the preparation of Co_3O_4 NPs,[163] known antimicrobial and antioxidant agents,[164] via calcination. Ca^{2+}/Co^{2+}-alginate beads induced human adipose-derived mesenchymal stem cells (hADSCs) differentiation into cartilage producing chondrocytes.[165]

Interestingly, TGA and FT-IR analysis indicate that incorporating Co^{2+}-alginate powder (produced by drying an hydrogel matrix) in epoxy resins increases the flame retardant properties of the latter.[166] Liu et al. deeply investigated this aspect, proving that crosslinking alginate with Co^{2+} ions accelerates the thermal degradation of the polymer chains (decarboxylation onset around 185 °C).[81] However, in the 180–340 °C range a lower amount of gaseous products was produced with respect to sodium alginate, confirming the previously mentioned flame retardancy.[81]

3.2.7. Nickel

The well-known risks associated with the use of Ni^{2+} (e.g., allergy, lung fibrosis)[167] significantly lowered the interest in Ni^{2+}-crosslinked hydrogels. Despite this, the distinctive properties imparted by this ion and the high stability of Ni^{2+}-alginate hydrogels still make them of interest to researchers.

Studies on the sol–gel transition of alginate induced by Ni^{2+} ions highlighted a second order kinetics for the process.[168] The resulting networks exhibited lower stability toward decarboxylation (onset ≈ 180 °C) with respect to sodium alginate, but superior flame retardant properties due to the reduced amount of gas released during thermal degradation.[169] XPS analysis of Ni^{2+}-alginate hydrogels performed by Zhang et al. showed that the Ni^{2+} binds to both carboxyl and oxydril groups of the alginate backbone.[69] DFT calculations also indicated that Ni^{2+} preferably coordinates 4 glycosidic units maintaining a distance of ≈1.9 Å from each oxygen/containing functional group (both in gas and water phase).[170]

Recently, Xiong et al. developed a device for cancer immunotherapy consisting of a histidine-tagged Interleukin 2 (IL2)

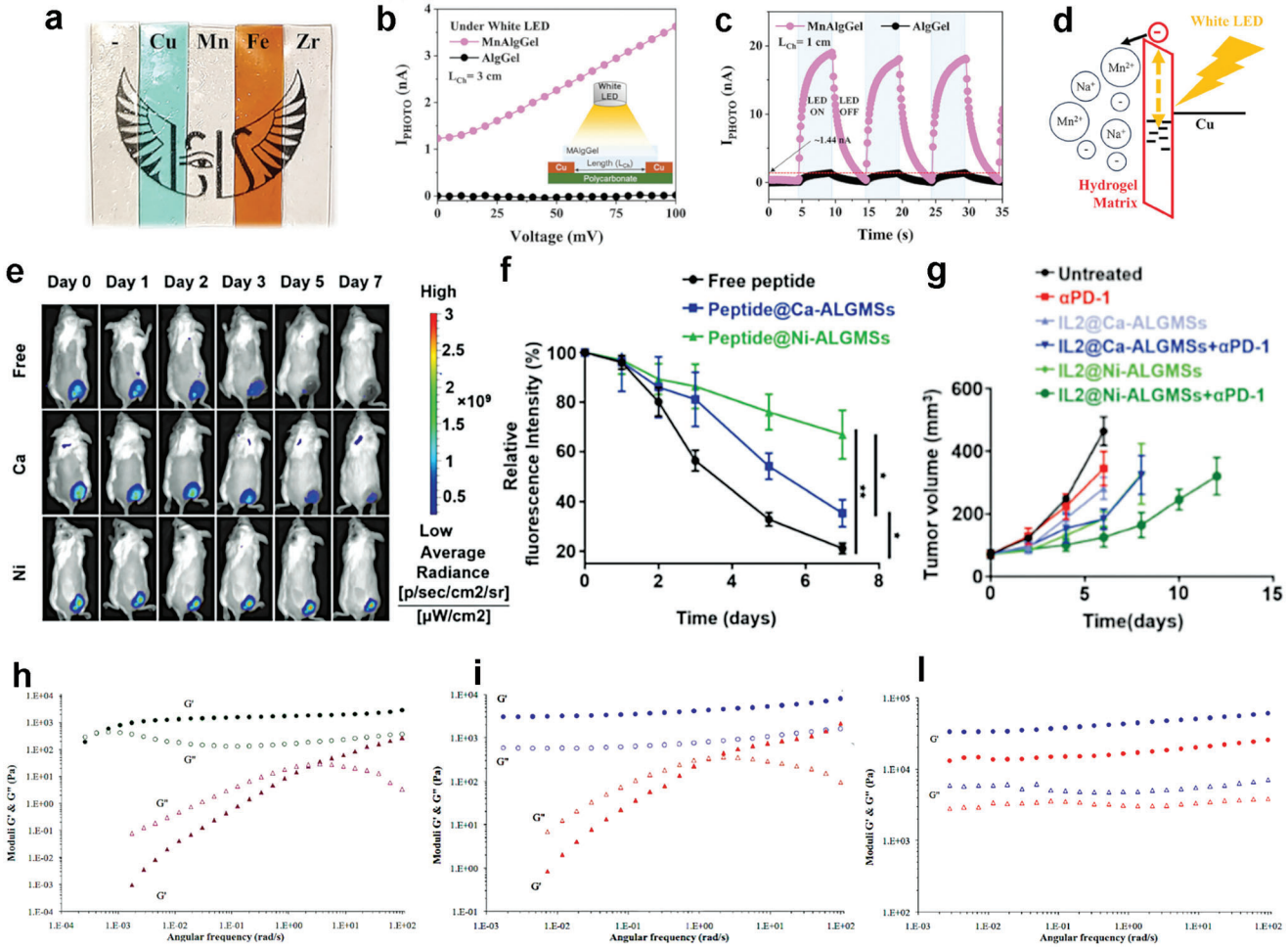

Figure 4. *First row:* photoresponsive ionic conductive M-alginate/gelatin (M = Cu, Mn, Fe, Zr) organohydrogels compared with their sodium alginate/gelatin (AlgGel) counterparts. Adapted with permission.[76] Copyright 2024, John Wiley and Sons. a) Optical image of the prepared MAlgGel samples placed on top of a printed logo. b) Photoresponse of MnAlgGel and AlgGel upon exposure to white LED. c) Time-resolved photoresponse of the MnAlgGel and AlgGel photodetector with a channel length of 1 cm. d) Band diagram of the MnAlgGel/Cu electrode interface. *Second row:* Injectable Interleukin 2 (IL2) loaded into Ni^{2+}-alginate microspheres for cancer therapy. Adapted with permission.[171] Copyright 2022, John Wiley and Sons. e) In vivo fluorescence imaging of mice after injection of free Cy5.5 labeled his-tagged peptide (Cy5.5-his-peptide), Cy5.5-his-peptide@Ca-ALGMSs, and Cy5.5-his-peptide@Ni-ALGMSs. f) The relative fluorescence at tumor areas from day 0 to day 7 postinjection of the above Cy5.5 labeled agents. g) Average B16-F10 tumor volumes of different groups during the treatment. *Third row:* influence of transition metal cations and guluronate content on the frequency-dependent viscoelastic properties of: h) Mn-HG (●/°) and Mn-LG (▲/△) alginates. i) Co-HG (●/°) and Co-LG (▲/△) alginates. l) Cu-HG (●/°) and Cu-LG (▲/△) alginates. G' (filled symbols) and G'' (open symbols)—G' (filled symbols) and G'' (open symbols)—T = 25 °C; σ_0 = 20 Pa. Adapted with permission.[72] Copyright 2014, Elsevier.

loaded into Ni^{2+}-alginate microspheres (Figure 4 highlights the results) thanks to the coordination to the metallic center. The formulation could be injected directly in the tumor, enhancing the production of inflammatory cytokines and minimizing the adverse effects caused by intravenous administration of the drug alone.[171]

The selectivity of Ni^{2+}-alginate hydrogels toward polyhistidine tags was reported also by Dumitraşcu et al.[172] It is noteworthy that calcination at 500 °C of Ni^{2+}-alginate beads resulted in the formation of single cubic phase nickel oxide (NiO) nanoparticles, thanks to the slow collapsing of the alginate network during the thermal treatment.[173]

Previously mentioned Zhang's XPS studies were instrumental to determine the favored binding sites of ciprofloxacin on Ni^{2+}-crosslinked alginate gels, in order to prove their suitability for the removal of this antibiotic from water.[69] Sami et al. reported that Ni^{2+}-alginate hydrogels can act as selective absorbents for lead (II) ions in water.[174] However, the ion exchange mechanism highlighted by the authors casts doubts on the utility of such products, as it can lead to the potential release of Ni^{2+} in the environment.

3.2.8. Copper

Rodrigues and Lagoa reported a lower selectivity of Cu^{2+} with respect to Ca^{2+} toward the alginate binding sites. Cu^{2+} absorption studies (Cu^{2+} concentration in the crosslinking solution, be-

fore and after gelation, was determined by molecular absorption spectroscopy) highlighted that the egg box coordination model[15] is verified only at low Cu^{2+} concentrations, while the number of interacting binding sites reduces to one or two at high crosslinker concentrations.[175] Viscometric and spectroscopic evaluations of Cu^{2+}-alginate diluted solutions support this binding modality.[176] Rheological tests on Cu^{2+}-alginate gels (with both low and high guluronate content) showed no flow regions ($G'' > G'$): this behavior, in contrast with Mn^{2+}- and Co^{2+}-alginate gels, suggests an atypical binding modality that results in networks with high cohesion.[72]

Small angle X-ray scattering (SAXS) analysis made it possible to monitor Cu^{2+}-induced alginate sol–gel transition, highlighting that copper prefers a less selective binding mode than the egg box.[68] SAXS was also useful in correlating the assembly at the molecular scale with the macroscopical mechanical properties. In fact, while the system's correlation length (ξ) remains unaffected by the Cu^{2+} concentration, the resulting hydrogels proved to be rigid enough to be suitable for the encapsulation of actives. Camacho et al. developed Cu^{2+}-alginate beads for folic acid encapsulation, enabling pH-responsive release: the hydrogels shrunk in acidic pH (e.g., in the stomach), while started to swell and release folic acid when pH was higher than 5. This device therefore allowed the release of folic acid in the intestinal environment, protecting the active during the previous path of the digestive system.[34]

Cu^{2+}-alginate complexes leverage copper's antimicrobial properties to prepare biocidal products. The treatment of wool and cotton cellulose fabrics with Cu^{2+}-alginate has been shown to impart antimicrobial properties durable after several washing cycles.[177,178] Cu^{2+}-alginate hydrogels' antimicrobial and drug encapsulation properties can be used to prepare scaffolds for bone tissue regeneration: Qi et al. demonstrated that cannabidiol loaded Cu^{2+}-alginate hydrogels exhibit antibacterial, anti-inflammation, angiogenic, and osteogenic activities and are beneficial for bone defects healing.[179] Additionally, Klinkajon et al. also highlighted that alginate hydrogels containing Cu^{2+} ions are suitable for antimicrobial wound dressing since they are capable of absorbing a high quantity of body fluids, enhancing prothrombotic coagulation and platelet activation.[180] Wound dressing hydrogels of that kind can be prepared by electrodeposition (gradually dissolving $Cu_2(OH)_2CO_3$ precursor), with excellent control over the structure and chemical composition (see **Figure 5**).[181]

The strong affinity of alginate for Cu^{2+} can be also exploited in the design of hydrogels with complex shapes: for example, wet spinning has been recently demonstrated as a viable and promising strategy to produce fibers.[78] Combined with its antimicrobial properties, the Cu^{2+}-alginate affinity could be extensively exploited for the preparation of inks for extrusion 3D printing, thereby expanding its application potential into additional technological fields.

Cu^{2+}-alginate hydrogels were employed as catalyst for the 1,3-dipolar cycloaddition of alkynes with azides and oxidative coupling of 2-naphthols and phenols in water.[182] For example, Bahsis et al. developed a reusable superporous hydrogel with high catalytic activity and regioselectivity (confirmed through DFT calculations) for the synthesis of 1,4-disubstituted-1,2,3-triazoles in water.[183] Souza et al. reported the preparation of a Cu^{2+}-alginate gel catalyst for the synthesis of 4-organylselanyl-1H-pyrazoles: the crosslinking strength contributes to the recyclability of the product (5 cycles tested).[184]

It is worth mentioning that CuAlg composites with polyacrylamide (PAM), obtained through radiation-induced polymerization of AM followed by alginate's ionic gelation, were found to effectively operate as highly stretchable ionic conductive strain sensors.[185] Application of Cu^{2+}-alginate gels always needs to take into account that Cu^{2+} ions strongly catalyze alginate chains degradation.[186]

3.2.9. Zinc

Zn^{2+}-alginate interaction, although being one of the weakest among the M^{2+}-alginate ones, has demonstrated significant potential for various applications, primarily due to the unique properties of this element. Viscometric characterization of Zn^{2+}-/Ca^{2+}-alginate diluted formulations proved that Ca^{2+} and Zn^{2+} do not compete for the same binding sites, suggesting that the egg box coordination[15] is inadequate to describe the Zn^{2+}-alginate complex.[187] Dynamic light scattering (DLS) analysis performed on diluted mixtures of alginate and zinc highlighted that the complexation process leads to the formation of alginate nanoparticles.[188]

Zn^{2+}-crosslinked alginate coatings can be used for diverse applications. For example, by leveraging the antifouling properties of zinc,[189,190] Nassif et al. developed an electrophoretic method for the preparation of uniform Zn^{2+}-crosslinked alginate coatings for stainless steel.[191] Additionally, due to the thermally induced conversion of Zn^{2+} ions to ZnO, Zn^{2+}-crosslinked alginate films proved to act as flame retardants.[192]

Zn^{2+}-alginate pyrolysis behavior strongly differs from that of sodium alginate: Liu et al. pointed out (using TGA, TG-FTIR, and pyrolysis-gas chromatography-mass spectrometry (Py-GC-MS)) that crosslinking with Zn^{2+} shifts the decarboxylation onset abundantly below 200 °C, while reducing the number of pyrolysis compounds (less flammable gaseous products).[80]

Zn^{2+}-crosslinked alginate beads have been shown to perform slow release of nitrogen-based fertilizers, due to the strong Zn^{2+}-alginate interaction, resulting in hydrogels with small porosities.[193]

Interestingly, Wen et al. developed zinc-ion hybrid supercapacitor (ZHS) based on a Zn^{2+}-alginate/PAAm hydrogel acting as electrolyte. This system is sensitive to applied pressures and allows easy modulation of energy density by adjusting Zn^{2+} concentration, suggesting its potential as a self-powered sensor for detecting human movement and breathing.[194] Zn^{2+}-alginate has also been used to enhance the electrochemical performance of Zn ion batteries: coating Zn electrodes with thermoplastic polyurethane (TPU) infiltrated with ZnAlg minimizes corrosion and dendrite growth.[195]

Zn^{2+}-alginate hydrogels with finely controlled morphologies can be prepared through internal gelation. D-(+)-gluconic acid δ-lactone (GDL) addition to $[ZnCO_3]_2{\cdot}[Zn(OH)_2]_3$-loaded alginate induces the progressive release of Zn^{2+} ions and produces a highly homogeneous network.[74] Gray et al. showed that Zn^{2+}-alginate hydrogels are suitable for performing slow insulin release. This evidence was attributed to

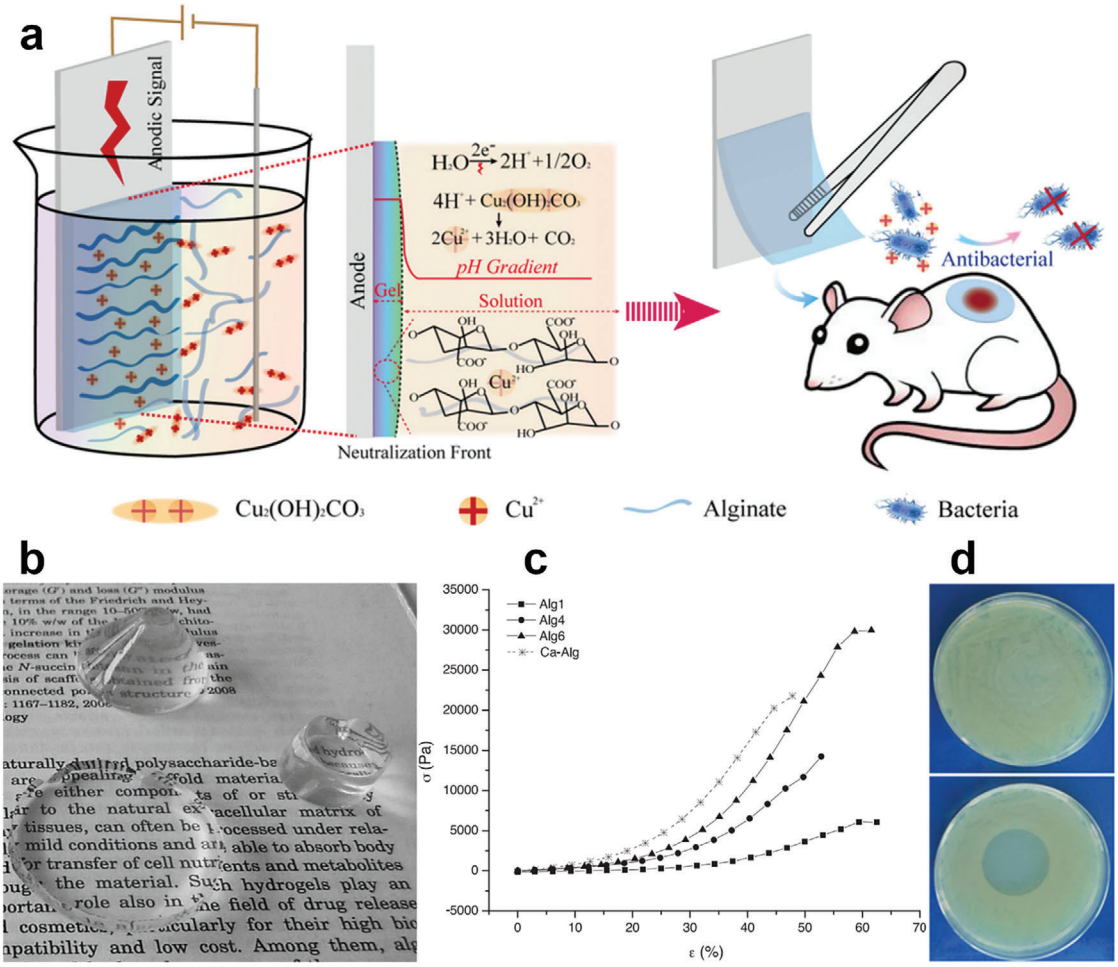

Figure 5. *First row:* a) Sketch of the preparation of antimicrobial Cu^{2+}-alginate dressing through electrodeposition. Adapted with permission.[181] Copyright 2021, Springer Nature. *Second row:* b) Transparent Zn^{2+}-crosslinked alginate gels obtained by internal gelation. Adapted with permission.[74] Copyright 2015, Elsevier. c) Stress versus strain curves of Zn^{2+}-alginate gels (Alg1, Alg4, Alg6) prepared under different pH conditions, compared to a Ca^{2+}-alginate reference. Adapted with permission.[74] Copyright 2015, Elsevier. d) Bacteria inhibition zones of Ca^{2+}-alginate (top) and Zn^{2+}-alginate (bottom) gels. Adapted with permission.[74] Copyright 2015, Elsevier.

the high density of the Zn^{2+}-crosslinked hydrogel structure with respect to Ca^{2+} and to a possible Zn^{2+}-insulin bridge formation.[196]

Interestingly Zn^{2+}-alginate formulations have been demonstrated to improve the stability of color and chemical composition of natural pigments from anthocyanin-rich purple corn extract, proposing a viable and sustainable opportunity for innovation in the beverage sector.[31]

3.2.10. Cadmium

Although Cd^{2+}-alginate interaction is one of the strongest among the M^{2+}-alginate complexes (leading to gels with high Young modulus[101]), the interest in this cation is strongly limited by its toxic nature.[197] The strong interaction is also why alginate is often exploited for the removal of Cd^{2+} contamination from water: alginate gel beads (sometimes in the form of organic/inorganic composite systems), either crosslinked or not, were profitably used for this purpose due to the fast ion exchange involving Cd^{2+} ions.[198–201]

Wang et al. developed Cd^{2+}-alginate nanobeads for triple tumor marker detection (Alpha fetoprotein, AFP; Carcinoembrionic antigen, CEA; Prostate specific antigen, PSA), using a double-water-in-oil-emulsion procedure.[202] The beads were used to immobilize labeled anti-AFP, anti-CEA, and anti-PSA and then immobilized on a conductive substrate. The presence of Cd^{2+} ions is crucial since they generate the anodic peaks necessary for analyte detection via differential pulse voltammetry (DPV).[202]

3.2.11. Lead

As previously introduced, the affinity between alginate and Pb^{2+} ions is the strongest among all divalent cationic species. Lamelas et al. studied the complexation between Pb^{2+} and alginate, mixing alginate and lead-containing solutions in various conditions

and using Pb^{2+}-selective electrodes:[203] authors highlighted that, in the pH 4.0–8.0 range, the uptake of lead ions by the alginate matrix is a linear function of the Pb^{2+} concentration in the bath, regardless of pH variations. Furthermore, cation-alginate complexation experiments (performed with variable ionic strength) proved that coulombic interaction accounts for 15% of the formation of the complex.[203]

As observed by Andresen and Smidsrød, the elasticity modulus (E) of Pb^{2+}-crosslinked alginate gels decreases as a function of the temperature (from 10 to 50 °C),[204] suggesting their potential use as thermoresponsive functional materials. The negative temperature dependence of E testifies that the entropy of the system increases during compression, likely due to the rupture of linkages in the organized hydrogel matrix.[204]

Due to the high toxicity of lead,[205] the strong interaction between Pb^{2+} and alginate is often exploited to remove the ion from water or gastric juices:[174,206] Ca^{2+}-alginate gels are suitable for this purpose, since the calcium can be easily replaced by lead in the polymeric network.[207,115]

3.2.12. Uranyl

This subsection is titled "Uranyl" rather than "Uranium" and it belongs to the divalent cations section because of a well-defined reason. In fact, although uranium has an oxidation state of (VI) in the uranyl cation, this cation behaves similar to divalent elements. A unique study of Hassan demonstrated that the interaction between alginate and uranyl cations (UO_2^{2+}) results in the formation of hydrogels.[208] Titrimetric analysis examined the competition between uranyl cations and protons for the carboxylate groups, revealing an equilibrium constant of ≈15.5 for the UO_2^{2+}-alginate complex. IR spectroscopy confirmed the coordination between UO_2^{2+} ions and the polymer backbone, evidenced by characteristic shifts of the $\nu(COO^-_{asym})$ and $\nu(COO^-_{sym})$ bands with respect to sodium alginate reference (to lower and higher energies, respectively).[208] This coordination with the uranyl groups also led to the appearance of a band at 930 cm^{-1}, absent in the sodium alginate spectrum. XRD diffraction patterns proved the amorphous nature of the UO_2^{2+}-alginate complex.[208] Two coordination geometries were proposed for the UO_2^{2+}-alginate complex. In the case of intrachain interaction, or "planar interaction," both hydroxyl and carboxylate groups are involved in the coordination. On the other hand, interchain interactions (see Figure 1b–d) involve only carboxylate groups from different polysaccharide chains, forcing the uranyl cations to arrange in a plane that is perpendicular to that of the polysaccharide chains (nonplanar geometry).

3.3. Trivalent Cations

Cr^{3+}, Fe^{3+}, Al^{3+}, Ga^{3+}, La^{3+}, Ce^{3+}, Eu^{3+}, Tb^{3+}, and Gd^{3+} form hydrogels through interactions with alginate chains. Their complexes typically exhibit octahedral geometries, where the binding of M^{3+} ions is predominantly intermolecular due to the reduced strain on the cation-oxygen bonds in this configuration.[209] The coordination involves two carboxyl groups from one alginate chain and one carboxyl group from another, resulting in asymmetrical attraction forces. Consequently, the formation of M^{3+}-alginate hydrogels takes place anisotropically, with a preferential direction, especially when diluted alginate solutions are used.[13]

Thermogravimetric studies by Zaafarany et al. on various alginate complexes have shown that the thermal stability of M^{3+}-alginate gels is cation-dependent, following the order (determined from the decarboxylation onsets): $Al^{3+} > Cr^{3+} > Fe^{3+}$.[210] M^{3+}-alginate complexes were also characterized through FT-IR spectroscopy, unraveling that the coordination of M^{3+} ions leads to shifts of the symmetric and asymmetric $-COO^-$ stretching bands with respect to sodium alginate.[209] The following sections will provide a detailed discussion for each of the trivalent cations mentioned above.

3.3.1. Chromium

The preparation of Cr^{3+}-alginate hydrogels was first reported and patented by Milin et al. in 2003,[211] although the interaction between alginate and Cr^{3+} ions was already known.[212] This material has been proposed for artificial chromium supplementation. Additionally, Cr^{3+}-alginate interaction can be exploited for Cr^{3+} removal from water. Araújo et al. demonstrated that Ca^{2+}-alginate gels are effective for this purpose, as they can load substantial quantities of Cr^{3+}, mainly through ion exchange.[212]

3.3.2. Iron

Fe^{3+} is the most extensively studied among the M^{3+} ions capable of crosslinking alginate due to its strong ionic interactions, which create stable and versatile hydrogels with desirable mechanical properties, biocompatibility, and functionality for various biomedical and industrial applications. Notably, Fe^{3+}-alginate hydrogels can be formed either using Fe^{3+} or Fe^{2+} salts as precursors. The latter approach is less common and requires the oxidation of the ions after the crosslinking.

Sreeram et al. proved through pH-metric titration that the complexation with alginate increases the stability of Fe^{3+} ions, preventing precipitation of ferric hydroxides till pH 4.2.[213] This aspect is particularly interesting since it suggests that Fe^{3+}-alginate could possibly replace chromium (III) ions in the leather industry, during the tanning process.[214]

Fe^{3+}-alginate crosslinked structures and derivatives demonstrated high application potential in the removal of water contaminants, such as Cr(VI) and As(III).[215–217] Zhang et al. developed an Fe^{3+}-alginate photocatalyst capable to concomitantly reduce Cr(VI) to Cr(III) and oxidize As(III) to As(V). The obtained products, beyond their lower toxicity with respect to their precursors, are easier to adsorb on the crosslinked polymeric structure.[218]

Furthermore, Fe^{3+}-alginate films have been shown to catalyze the decolorization of methyl orange through Fenton-like processes, with good recyclability.[219] The ease of reducing Fe^{3+} to Fe^{2+} via UV irradiation—with a consequent reorganization of the alginate chains—enables to obtain photoresponsive Fe^{3+}-alginate composites, suitable as soft actuators.[220]

It is worth mentioning that, as described by Liu et al., replacing sodium with iron strongly improves the flame retardant properties of alginates, achieving an excellent V-0 rating

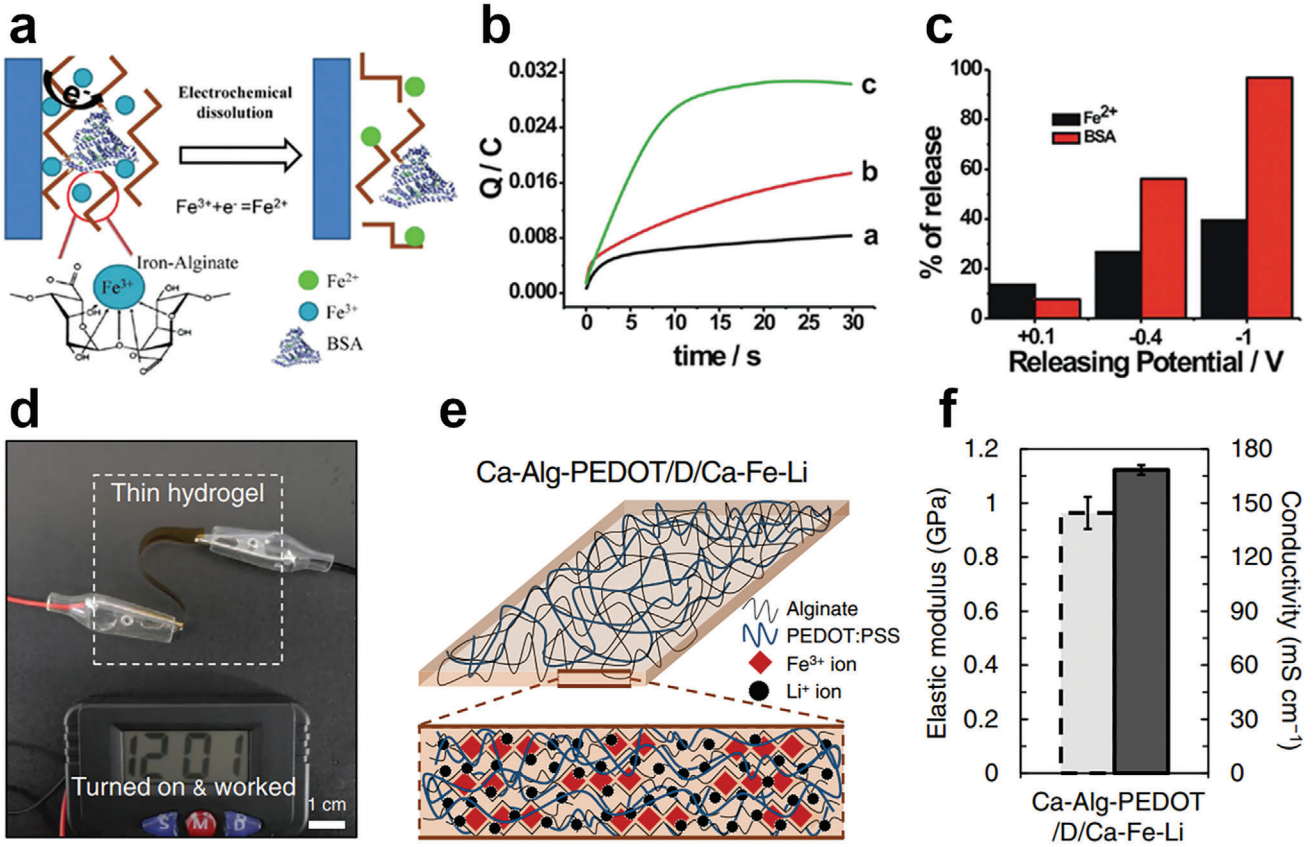

Figure 6. *First row:* a) Scheme of the electrochemically induced BSA release from Fe^{3+}-alginate scaffold.[226] b) Chronocoulometry curves obtained for the electrochemical dissolution of the BSAFeAlg films upon application of different reductive potentials: a) +0.1, b) −0.4, c) −1.0 V to the modified electrode. Adapted with permission.[226] Copyright 2011, American Chemical Society. c) Percentage (from the total amount in the BSAFeAlg film) of the released iron cations and BSA upon application of different reductive potentials for 30 min. Adapted with permission.[226] Copyright 2011, American Chemical Society. *Second row:* d) Demonstration of the stable working performance of Ca–Alg/D/Ca–Fe–Li hydrogels solid gel electrolytes. e) Schematic structure of the Ca–Alg–PEDOT/D/Ca–Fe–Li hydrogel matrices. f) Elastic modulus and conductivity of Ca–Alg-PEDOT/D/Ca–Fe–Li hydrogels. Adapted with permission.[122] Copyright 2022, Springer Nature.

in the UL-94 test (i.e., the Standard for Safety of Flammability of Plastic Materials for Parts in Devices and Appliances testing), making iron alginate an inherent flame-retardant material.[79]

Fe^{3+}-alginate photodegradable gels were produced by Narayanan et al.,[221] following this procedure in order to obtain a homogeneous distribution of cations in the network. These gels, when supplemented with sodium lactate, showed to be photodegradable if exposed to UV light (λ = 365 nm) and therefore suitable for biomedical applications.[221]

Fe^{3+}-alginate films have shown significant potential as tissue engineering scaffolds due to their superior protein adsorption properties (especially vitronectin) with respect to Ca^{2+}-alginate films, supporting fibroblast adhesion, spreading, and proliferation.[222] Machida-Sano et al., corroborated fibroblast adhesion, noting that the phenomenon becomes more favorable as the alginate's guluronate content increases.[223] Fe^{3+}-alginate gels have been also proposed as carriers for the release of DNA fragment[224] or proteins (e.g., lysozyme and BSA).[225,226] In this latter case, Jin et al. demonstrated that electrochemical reduction of the Fe^{3+} ions allows the modulation of the drug release profile, due to the lower stability of the Fe^{2+}-alginate crosslinked network (**Figure 6**).

3.3.3. Aluminum

Due to the high affinity between Al^{3+} and fluoride ions, Al^{3+}-alginate gels were proposed for the removal of fluoride (F^-) from water by the groups of Kaygusuz[227] and Zhou.[228] Both papers describe devices with intriguing properties, even though some details are still to be fully addressed, such as the effect of pH on the carboxylate stretching bands of alginate.

Al^{3+}-alginate hydrogels have also been suggested as carriers for drug delivery,[229,230] although their use in this field is limited compared to other cations (e.g., Ca^{2+}).

In addition to Fe^{3+} ions, Liu et al. also investigated the effect of Al^{3+} ions on the thermal degradation mechanism of alginate, using TGA-FTIR-MS and Py-GC-MS: Al^{3+} ions proved to favor dehydration, decarboxylation, and decarbonylation of alginate.[231] This study is particularly relevant in the view of the use of Al^{3+}-alginate gels as flame retardants.

Yang et al. demonstrated that Al^{3+}-mediated crosslinking of alginate/polyacrylamide hydrogels significantly enhances the mechanical properties of the matrix making it suitable for use as a vibration isolator.[232]

3.3.4. Gallium

Ga^{3+}-alginate gels are well-known for their antimicrobial properties, as recently highlighted by Li et al.[233] This antimicrobial efficacy can be attributed to the similarity between Ga^{3+} and Fe^{3+} ions, which allows Ga^{3+} to interact with iron-binding proteins, thereby disrupting iron-dependent metabolic pathways in bacteria.[234,235] Rasting et al. demonstrated that gallium-mediated crosslinking imparts significant antimicrobial activity and compressive strength to alginate-containing inks for 3D bioprinting.[235] The resulting scaffolds were capable of maintaining the viability of encapsulated fibroblasts over 90% for 7 days. It is worth mentioning that composites comprising Ga^{3+}-alginate and bioactive glass exhibited promising properties for bone tissue engineering application.[35,236]

3.3.5. Yttrium

Y^{3+} ions are reportedly capable of interacting with alginate carboxylate groups[237] leading to crosslinking phenomena. However, Y^{3+}-crosslinked alginate scaffolds have not garnered particular attention and their applications are limited to water purification. Electrostatic interaction and hydrogen bonding between pollutants and yttrium ions were found to be the main factors responsible for the efficiency of Y^{3+}-alginate beads in the removal of dyes[238,239] and fluoride ions.[240] As proved by He et al. through XPS characterization, F^- ions have the ability to replace the hydroxide groups bonded to the Y^{3+}.[239]

3.3.6. Lanthanides

Despite the high cost of lanthanide salts, research on alginate complexations persists due to the unique properties these complexes offer, such as in bioimaging and sensing applications. This ongoing interest is summarized in the following subsections and it reflects the significant potential and value of these materials.

Lanthanum: The high cost of lanthanum-based salts limits the study of La^{3+}-alginate gels. However, due to the strong affinity between La^{3+} and phosphate (PO_4^{3-}) ions,[241] several studies regarding La^{3+}-alginate matrix for PO_4^{3-} removal are reported. In most of them La^{3+}-alginate hydrogels were dehydrated[242,243] or even calcined[244] before use. Liu et al. proposed a composite La^{3+}-alginate-attapulgite (an aluminum silicate clay[245]) hydrogel adsorbent for PO_4^{3-} ions removal from water.[244] The system gained mechanical strength and stability from attapulgite, while the sorption properties primarily derived from the La^{3+}-crosslinked polymer matrix.[244] Additionally, Li et al. proved that La^{3+}-alginate beads can efficiently remove azo-dyes from water, mainly due to electrostatic and hydrogen bonding interactions.[246] The coordination between La^{3+} and alginate carboxylic groups was confirmed through FT-IR spectroscopy, as evidenced by the shift of the asymmetric —COO^- stretching band to higher energies.[246]

Cerium: Ce^{3+} complexes with alginate have been relatively underrepresented in literature, primarily due to the high cost of cerium salts. Nonetheless, investigations have revealed robust interactions between Ce^{3+} ions and alginate chains, resulting in densely packed structures with high thermal stability (i.e., main degradation in 700–850 °C range).[247] Interestingly, DFT calculations highlighted the Ce^{3+}-alginate interaction is more favorable than the Cu^{2+}-alginate one.[247] Ce^{3+}-alginate complexes have been proposed for corrosion protection applications, leveraging the facile substitution of Ce^{3+} ions by the common ions produced during corrosion processes (e.g., Fe^{3+}, Fe^{2+}, Al^{3+}, and Cu^{2+}) while exhibiting low toxicity profiles.[248] Moreover, the affinity between Ce^{3+} and fluoride (F^-) ions can be exploited for the design of crosslinked scaffolds for water purification purposes.[249] In the biomedical sector, Ce^{3+}-alginate beads have demonstrated wound healing capacities owing to their antimicrobial character (evaluated against *Staphylococcus aureus* and *Escherichia coli*).[250]

Neodymium: Nd^{3+} ions attracted significant interest for in vivo applications, due to their low toxicity[251] and high fluorescent emission intensity when complexed with alginate.[75] Additionally, Nd^{3+}-alginate scaffolds showed impressive mechanical properties, surpassing those of their Ca^{2+}-based counterparts.[75] Huang et al. exploited the affinity of Nd^{3+} toward alginate carboxylate groups to develop crosslinked alginate-(carboxyl-functionalized graphene) composites with high tensile strength and solvent resistance.[252] Konishi et al. described in detail the ion exchange process that leads to the sorption of Nd^{3+} on alginic acid particles, highlighting its reversible nature[253]: Their findings indicated that the sorption process is predominantly governed by the rate of ion exchange between H^+ and Nd^{3+}, with external mass transfer and intraparticle diffusion playing negligible roles.[253]

Europium and Terbium: Ma et al. developed Eu^{3+}- and Tb^{3+}-alginate hydrogels capable of emitting red and green light, respectively (see **Figure 7**), when exposed to UV radiation.[254] FT-IR spectroscopy revealed shifts to higher energies in both the asymmetric and the symmetric —COO^- stretching bands as a consequence of the coordination between alginate and the M^{3+} center. The fluorescent emission of these hydrogels proved to be sensitive to the presence of the anthrax biomarker sodium dipicolinate (NaDPA), with low detection limits (8.3×10^{-8} M for Eu^{3+}-alginate and 9.0×10^{-8} M for Tb^{3+}-alginate).[254]

Gadolinium: Podgórna et al. developed Gd^{3+}-alginate nanogels through a reverse oil in water emulsion method, highly stable in suspension.[255] The formulation is a promising contrast agent since it demonstrated to be nontoxic for human neuroblastoma cells line SH-SY5Y and capable of shortening the T1 relaxation time in magnetic resonance imaging (MRI).[255]

3.4. Tetravalent Cations

The group of tetravalent cations did not attract particular interest and therefore solely two M^{4+}-alginate are described in the following paragraphs. It is worth mentioning that, as suggested by Hassan, tetravalent ions are restricted to crosslinking via intermolecular association: M^{4+} ions chelate two adjacent carboxylate groups from one chain and two from another.[13] This complexation mechanism results in identical attraction forces be-

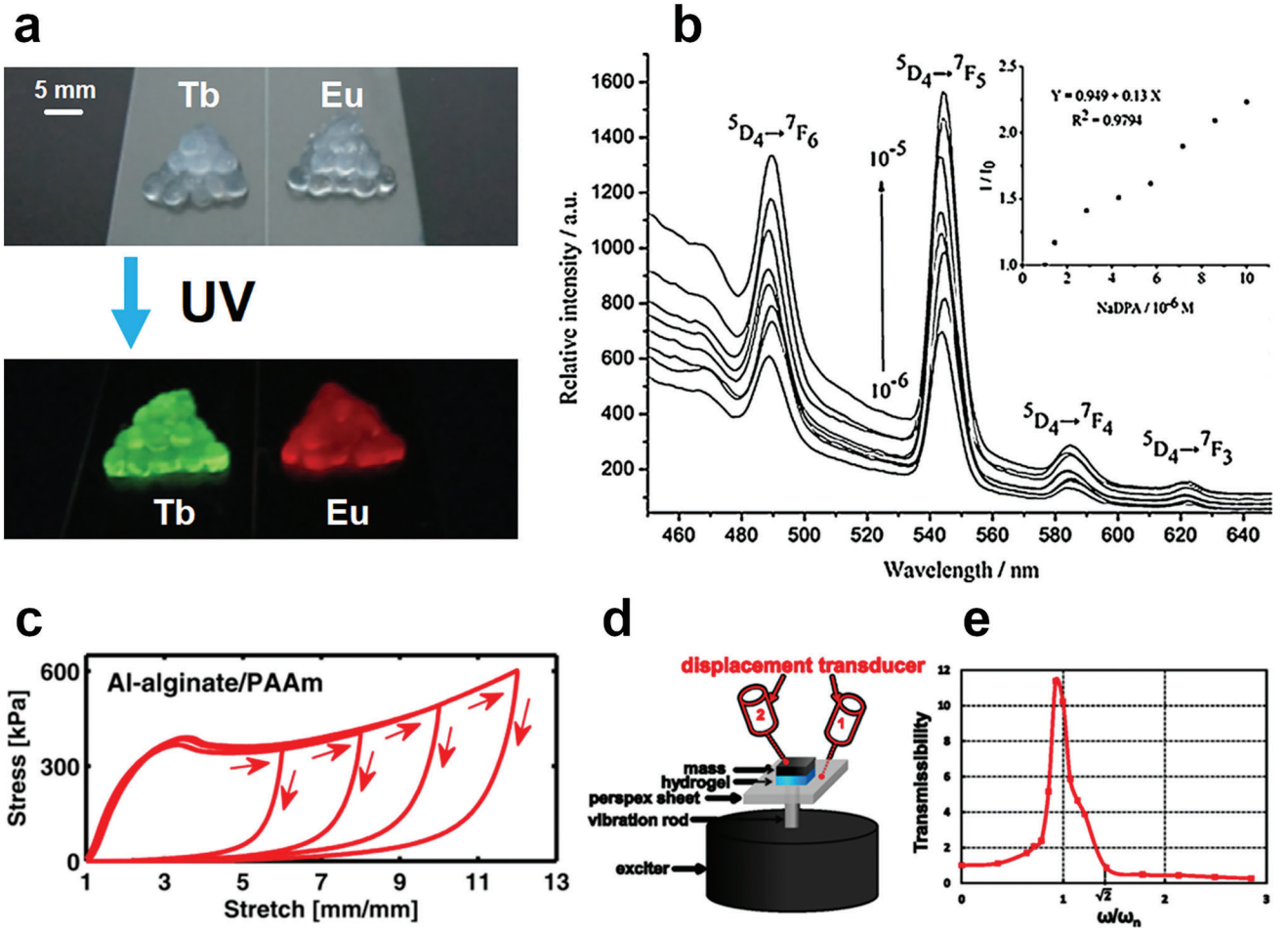

Figure 7. *First row:* a) UV light-sensitive Eu^{3+}- and Tb^{3+}-alginate hydrogels. b) Emission spectra ($\lambda_{ex} = 275$ nm) of the Tb^{3+}-alginate beads in the presence of different concentrations of NaDPA, from 10^{-6} M to 10^{-5} M. Adapted with permission.[254] Copyright 2015, Elsevier. *Second row:* c) Hysteresis curves of various kinds of alginate/PAAm hydrogels under stress. d) Scheme of the vibration isolation experiment set-up and e) transmissibility versus frequency ratio ω/ω_n. Adapted with permission.[232] Copyright 2013, American Chemical Society.

tween the ion and the carboxylate groups in all direction, potentially explaining the spherical symmetry and favorable mechanical properties of M^{4+}-alginate gel droplets, regardless of the alginate concentration.[13]

3.4.1. Zirconium

The high positive charge of Zr^{4+} facilitates the formation of strong interactions with the alginate chains, resulting in the formation of hydrogel networks. This charge was also reported to be responsible for an easy hydrolysis of the metal center and formation of a solvation sphere, beneficial for the coordination of polluting species.[256] Li et al. developed magnetic Zr^{4+}-alginate hydrogels with high efficiency and reusability for the removal of Pb^{2+} ions.[256] Due to their high electron density, phosphate (PO_4^{3-}), fluoride (F^-), and nitrate (NO_3^-) ions interact with Zr^{4+} active sites and therefore can be easily adsorbed onto Zr^{4+}-crosslinked alginate beads.[257–259] To enhance the adsorption capabilities, fillers (e.g., graphene oxide and kaolin[258,259]) are commonly added. Interestingly, Zr^{4+} ions can be used for the preparation of crosslinked alginate fibers, adopting a wet spinning approach:[260] Zr^{4+}-alginate fibers developed by Chen et al. are capable of performing methylene blue removal from water, showing good recyclability. Due to the acid character of the Zr^{4+} crosslinking bath, the polymer network is partially protonated (highlighted through FT-IR spectroscopy).[260] This aspect is often neglected or misinterpreted (i.e., wrong FT-IR spectra assignment), although it plays a crucial role in the swelling properties (and on the water purification performances, as a consequence) of Zr^{4+}-alginate hydrogels.

3.4.2. Thorium

Zaafarany et al. demonstrated that Th^{4+} ions can effectively serve as crosslinkers for the formation of alginate hydrogels.[261] Titrimetric studies highlighted that the coordination of Th^{4+} ions is thermodynamically favorable, while IR spectroscopy revealed that Th^{4+}-alginate interactions determine a shift to higher en-

ergies of both the asymmetric and symmetric —COO^- stretching bands ($\nu(COO^-_{asym})$ and $\nu(COO^-_{sym})$, respectively).[261] Furthermore, the chelation of Th^{4+} by the alginate backbone was evidenced by the emergence of a band at 890 cm^{-1}. An interchain association mechanism—the only one enabling an octahedral coordination between (tri/tetra)valent cations and alginate—was proposed for the coordination of Th^{4+} ions.[261] As extensively known, thorium is a radioactive element and therefore the interaction with alginate can be used only for its removal (e.g., from water). Ding et al. developed alginate-immobilized *Aspergillus niger* microspheres (AAM) to perform thorium (IV) removal from water.[262] Like in the aforementioned Zaafarany's study, alginate $\nu(COO^-_{asym})$ IR absorption band shifted to higher energies in the presence of Th^{4+}, testifying the coordination: the ionic exchange mechanism contributes to increase the amount of loaded contaminant.[262]

3.5. Key Insights into Complexation and Hydrogel Properties

The information in this section is summarized in Tables 1 and 2, which provide valuable guidance for less experienced readers in shaping future research strategies on advanced alginate-based functional materials. Table 1 details the specific features of M^{X+}-alginate complexation and the intrinsic properties of the resulting hydrogel matrix, while Table 2 outlines the sectors that could benefit from the use of these complexes. For instance, Ca^{2+}-alginate is commonly applied in drug delivery and the food industry due to its nontoxic nature (even at high crosslinker concentrations), while Cu^{2+}-alginate is preferred for antimicrobial and catalytic applications because of its high reactivity. Lanthanides, with their intrinsic fluorescence, present promising opportunities for applications in sensing technologies and medical imaging. The precise description of the M^{X+}-alginate interactions reported in Table 1 is crucial to understanding why certain ions are selected for the specific applications shown in Table 2. It is also important to recognize that the complexation process and the hydrogel matrix properties are strongly affected by environmental conditions. Increased ionic strength can introduce competition during complexation, while temperature changes can influence the viscosity of alginate solutions and the diffusion rate of the crosslinker within the polymer network, both of which can lead to significant alterations in the crosslinked matrix properties. Furthermore, low pH levels can greatly affect the characteristics of alginate-based materials by inducing protonation of the alginate chains, thereby increasing rigidity and hydrophobicity of the network. This phenomenon commonly occurs while using Fe^{3+}, Al^{3+}, or Zr^{4+} as crosslinkers, as clearly mentioned in Table 1.

4. Functional Applications of Cation-Alginate Complexes: Current Technologies and Future Directions

Cation-alginate complexes serve as unique building blocks for advanced functional materials. Their strength derives not only from the inherent properties of the cation and alginate but also from the distinctive structures that form when alginate assembles around the cation. This dynamic interplay greatly enhances their versatility, making them highly effective in applications ranging from drug delivery and environmental remediation to sensing and energy storage.

Overall, while cation-alginate complexes hold great promise across various applications, significant challenges related to stability, performance, and scalability must be addressed to unlock the full potential of cation-alginate complexes, driving technological advancements in diverse fields.

This section examines these challenges in depth and in a broader context, proposing strategies to overcome them by building on advanced processing techniques and focusing on technological innovations. The content is organized to guide the reader through both well-established and less conventional application fields, emphasizing the potential of cation-alginate complexes in each area while highlighting the challenges that must be addressed for real-world application. Table 2 summarizes the functions, sectors of impact, and involved cations, along with relevant examples from the literature. It serves as a roadmap for researchers who may not yet be fully aware of the potential applications of cation-alginate complexes. While consulting Table 2, readers are encouraged to refer to Table 1 to gain a complete understanding of the physicochemical properties that determine the suitability of different ions (and related crosslinked alginate networks) for specific applications.

4.1. Food Additive and Supplements

Cation-alginate complexes are utilized in food products and supplements to enhance texture, stability, and nutritional value (e.g., preventing oxidation).[29–31,128–131,264,265] However, their effectiveness can be inconsistent due to sensitivity to processing conditions like temperature, pH, and moisture. This variability can affect the performance and stability of these complexes throughout a product's shelf life. Achieving desirable sensory qualities without compromising taste or texture is also a significant challenge.

In food supplements, managing the controlled release of encapsulated nutrients is essential to ensure bioavailability. Environmental factors can disrupt this control, leading to variable outcomes, and protecting sensitive nutrients during processing and storage remains crucial.

Innovative processing techniques can address these issues. Spray-drying produces more uniform alginate particles, enhancing consistency and stability. Advanced encapsulation methods, including freeze-drying and supercritical fluid processing, offer additional protection for nutrients and optimize release profiles, making cation-alginate complexes more reliable in food applications.

4.2. Biomedical Applications

Due to their well-known biocompatibility, mechanical stability, and capacity to retain large amounts of fluids, cation-alginate complexes hold significant promise in various biomedical applications, including their use as contrast agents in imaging, scaffolds for tissue engineering, drug delivery systems, and wound healing.[266–286] However, the successful implementation of these applications faces several challenges, such as ensuring

biocompatibility, minimizing toxicity, achieving precise mechanical properties, and controlling the release and stability of therapeutic agents.

In imaging, the careful selection and combination of cations can optimize contrast, enhancing image clarity while minimizing potential side effects. The biocompatibility of these complexes is crucial, as any toxicity could limit their use in clinical settings. Developing formulations that maintain high contrast while reducing adverse effects remains a key area of research.

In tissue engineering, advanced fabrication techniques like electrospinning improve scaffold integrity, supporting cell growth and tissue regeneration. However, achieving the necessary mechanical properties is challenging, as the scaffold must be strong enough to provide structural support while being porous enough to allow cell infiltration and nutrient exchange. Advanced fabrication techniques, such as electrospinning, can improve the integrity of these scaffolds, enhancing their ability to support cell proliferation and tissue integration.

In drug delivery, controlling the release and stability of encapsulated drugs is essential to ensure therapeutic efficacy. The modification of alginate structures, combined with innovative encapsulation methods like spray-drying, can enhance the stability of the complexes and provide more predictable release profiles. This approach can be particularly effective in delivering and releasing pharmaceuticals products over extended periods, improving patient outcomes.

Wound healing is another promising application of cation-alginate complexes. These materials can be used to create dressings that promote healing by maintaining a moist environment, absorbing exudates, and delivering antimicrobial agents directly to the wound site. However, challenges such as ensuring the optimal release of therapeutic agents or maintaining the structural integrity of the dressing over time are still to be addressed. The incorporation of bioactive cations and the use of advanced processing techniques can enhance the healing properties of these dressings, offering better control over drug release and improving the overall effectiveness of the treatment.

By addressing these challenges through innovative strategies, cation-alginate complexes could become vital tools in the development of next-generation biomedical materials. These materials have the potential to provide new solutions for imaging, tissue regeneration, targeted drug delivery, and wound healing, significantly advancing patient care and treatment outcomes.

4.3. Artificial Skins and e-Skins

Cation-alginate complexes offer promising potential for artificial skin applications due to their biocompatibility and flexibility.[76,127,287–289] However, several challenges need to be addressed to optimize their performance. Achieving a balance between flexibility and mechanical strength represents a major challenge. Cation-alginate materials can sometimes be too rigid or excessively soft, affecting their effectiveness as artificial skin. Additionally, maintaining consistent performance over time is crucial, as degradation due to moisture, UV exposure, or mechanical stress can compromise the material.

Another critical factor is the adhesion properties of these materials. For artificial skin to function effectively, it must adhere securely to underlying tissues without causing irritation or detachment over time. Poor adhesion can lead to slippage, discomfort, or compromised healing, particularly in dynamic or high-movement areas of the body.

In the context of electronic skins (e-skins), cation-alginate complexes can be further enhanced to exhibit sensor and super-capacitive properties, making them suitable for advanced biomedical and wearable technologies. These e-skins require materials that not only mimic the flexibility and durability of natural skin but also integrate functionalities, such as pressure sensitivity, temperature responsiveness, and energy storage. By incorporating conductive nanomaterials and optimizing the crosslinking processes, cation-alginate complexes can achieve the necessary electrical conductivity and mechanical resilience, enabling the development of multifunctional e-skins that can monitor physiological signals or power small devices.

To overcome these issues, enhancing the mechanical properties of cation-alginate materials through chemical modifications and the incorporation of reinforcing agents, such as elastic polymers or fibers, can improve both flexibility and strength. Advanced fabrication techniques like additive manufacturing enable precise layering and customization, allowing for a closer mimicry of natural skin. By employing these strategies, cation-alginate complexes can be developed into highly effective artificial skins suitable for various applications.

4.4. Antimicrobials

Cation-alginate complexes have potential as antimicrobial agents due to their ability to bind and, in certain conditions, release antimicrobial cations like silver or copper.[74,177,178,233,250] However, bottlenecks such as inconsistent ion release and resistance development need to be overcome. Controlling the release of these cations is crucial to avoid inadequate antimicrobial activity or excessive release leading to cytotoxicity. The potential for resistance development also limits the long-term effectiveness of single-ion antimicrobial agents.

Future research should focus on multication complexes that combine various antimicrobial mechanisms to reduce resistance likelihood. Balancing the release rates of multiple cations while maintaining biocompatibility is essential. Innovative processing techniques, such as spray-drying and electrospinning, could be utilized to produce antimicrobial devices with controlled morphology, composition and release, enhancing their performance and reducing resistance development.

4.5. Remediation by Complexation/Filtration

Owing to their biodegradability, recyclability, and high charge density, cation-alginate complexes are highly effective in environmental remediation, particularly for capturing heavy metals and other contaminants.[69,115,150,238,290–294] However, their broader application is challenged by limited selectivity, the capacity to handle multiple contaminants, and difficulties in regeneration and reuse.

To solve these problems, implementing ion-specific protocols during the remediation process (such as the use of competitive

complexing agents) could significantly enhance the efficiency of cation-alginate complexes. By tailoring the remediation strategy to target specific ions under certain environmental conditions, it is possible to optimize the uptake of particular contaminants while minimizing interference from others. This approach can improve the selectivity and overall performance of the complexes in diverse and complex environmental matrices.

Enhancing the physical stability of cation-alginate complexes is also critical. Techniques such as crosslinking alginate with other polymers or applying advanced surface coatings can increase the resistance of these complexes to leaching and degradation, ensuring they maintain functionality over extended periods. This enhancement would make them more viable for long-term remediation applications. Additionally, innovative processing methods like spray-drying or electro-spinning can produce structures with improved stability and increased surface area. This not only improves contaminant capture efficiency but also facilitates the handling and reuse of the complexes, addressing a significant obstacle to the widespread adoption of cation-alginate complexes in environmental remediation. By focusing on these solutions, cation-alginate complexes could become more effective and sustainable tools for environmental cleanup, offering improved performance and more immediate practical applicability in real-world scenarios.

4.6. Sensors

Cation-alginate complexes show promise in sensor applications (due to their sensitivity to the surrounding environment)[76,125,295,296] but their widespread use is still hampered by their limited sensitivity and selectivity, particularly in detecting low concentrations of analytes in complex environments. The weak and nonspecific interactions between alginate complexes and target molecules often result in false positives or reduced detection limits, undermining the reliability of these sensors. Another significant challenge is the slow response time of cation-alginate-based sensors, which restricts their effectiveness in real-time monitoring applications.

To overcome these limitations, enhancing the specificity of cation-alginate sensors is crucial. One promising approach involves the incorporation of selective recognition elements, such as molecularly imprinted polymers (MIPs) or aptamers, into the alginate matrix. These elements can provide higher binding affinities for specific target molecules, reducing the likelihood of false positives and improving the overall sensitivity of the sensor.

Innovative fabrication techniques also offer potential solutions. Additive manufacturing, for example, could enable the creation of sensor platforms with complex geometries and integrated microfluidics. These advanced designs could optimize the interaction between the sensor surface and the analyte, leading to faster response times and improved detection capabilities. By incorporating microfluidic channels, sensors could be designed to rapidly transport analytes to the detection site, thereby reducing the time required for a response.

Spray-drying and electro-spinning are other techniques that could be utilized to produce sensor particles with controlled size, shape, and surface properties. This level of control can enhance the interaction between the sensor and the analyte, improving both sensitivity and response time.

4.7. Supercapacitors

Cation-alginate complexes hold significant potential for energy storage applications, especially in supercapacitors,[122,269,297,298] where they function as dielectrics with high ionic content. However, challenges such as low energy density, poor cycle stability, and the inherently low conductivity of alginate have limited their performance in high-energy applications.

To overcome these limitations, several promising solutions are being explored. Integrating conductive additives, such as carbon black, metal nanoparticles, or conductive polymers, into cation-alginate complexes can significantly enhance their electrical conductivity. This approach can help to bridge the gap between the insulating nature of alginate and the high conductivity required for effective supercapacitor electrodes.

Combining alginate complexes with advanced materials like graphene or carbon nanotubes offers another powerful strategy. These materials are known for their exceptional electrical properties and mechanical strength, making them ideal components for improving both the conductivity and structural integrity of alginate-based supercapacitor electrodes. By creating hybrid materials that leverage the strengths of both alginate and these high-performance additives, researchers can achieve better energy density and cycle stability, extending the lifespan and efficiency of the supercapacitors.

Innovative processing techniques also play a crucial role in enhancing supercapacitor performance. Additive manufacturing, for instance, can be used to create complex, layered architectures that optimize ion transport within the electrode structure. By precisely controlling the arrangement and composition of the layers, it is possible to maximize the surface area available for charge storage while ensuring efficient ion movement, which is key to improving the overall performance of the supercapacitor.

By focusing on these solutions, cation-alginate complexes could become more viable and effective materials for next-generation supercapacitors, offering enhanced energy density, better cycle stability, and greater overall efficiency in energy storage applications.

4.8. Catalysts

Cation-alginate complexes are emerging as promising candidates for catalytic applications (leveraging their recyclability and biodegradability) in green chemistry,[182–184,299–301] but their effectiveness is often constrained by several key challenges. One significant issue is their stability and activity under harsh conditions: in fact, the structural integrity of alginate complexes can degrade over time, particularly when exposed to high temperatures or extreme pH levels.

Several strategic improvements should be adopted to overcome these limitations. Enhancing the robustness of cation-alginate complexes is crucial. By selecting cations known for their stability and catalytic efficiency, the longevity and performance of the complexes can be significantly improved. Additionally, chemically modifying the alginate matrix—for example by making use

of crosslinking or grafting with more resistant polymers—can enhance its resistance to degradation and improve overall stability.

Innovative fabrication techniques offer additional solutions to enhance catalytic performance. Additive manufacturing allows for the creation of catalytic structures with precise geometries, which can enhance the exposure of active sites and optimize mass transfer. Spray-drying is another valuable technique for improving the performance of cation-alginate catalysts. By producing finely divided particles with controlled morphology, spray-drying enhances the dispersion of the catalytic material and increases its surface area, leading to improved catalytic activity. This method can also contribute to more uniform particle sizes, which further optimizes the performance of the catalysts. Electrospinning provides a promising approach for producing high-surface-area devices. This technique generates fibrous materials with a large surface area relative to their volume, potentially increasing the overall efficiency of the catalytic process.

4.9. Flame Retardants

Cation-alginate complexes show promise as sustainable flame retardants,[80,144,166,169,302–306] due to the significant amount of residue produced during combustion. However, their practical application is hindered by several challenges. One major issue is that incorporating these complexes often compromises the mechanical properties of the materials they protect. The addition of cation-alginate complexes can lead to increased brittleness or reduced strength, which can significantly affect the durability and usability of the materials.

Achieving uniform distribution of cation-alginate complexes within the host material also represents a difficult target. Poor dispersion can result in uneven flame retardancy, where some areas may not receive adequate protection. This inconsistency can undermine the effectiveness of the flame retardant and limit its practical applications.

Addressing these challenges requires targeted strategies. Improving the compatibility of cation-alginate complexes with various matrices is essential. Surface modifications to the alginate or the use of synergistic additives can enhance both flame retardancy and mechanical properties. For instance, incorporating additives that strengthen the material while preserving its flame retardant capabilities can help balance these conflicting requirements. Innovative fabrication techniques offer additional solutions. Additive manufacturing enables the precise incorporation of cation-alginate complexes into materials, which can improve uniformity and integration.

4.10. Mechanical Isolators

Cation-alginate complexes hold potential as mechanical isolators due to their flexibility, tunable mechanical properties, and lightweight nature.[232] However, optimizing their performance requires addressing several challenges.

Above all, achieving effective mechanical isolation is particularly complicated. Cation-alginate materials must become capable of absorbing and dissipating vibrations and shocks without compromising their structure. Current formulations may not always provide adequate isolation or can suffer from degradation when placed under stress.

Uniformity in performance is also critical. Heterogeneous distribution of the complexes can lead to areas featuring inadequate isolation. Additionally, the material must maintain its performance across various temperatures and environmental conditions.

Adhesion properties are equally important for the efficacy of cation-alginate isolators. Ensuring strong adhesion between the cation-alginate complexes and the substrates they are applied to is crucial for maintaining mechanical stability. Moreover, reversible adhesion, where the materials can be adhered and detached multiple times without significant loss of performance, can enhance the sustainability of these isolators. This capability allows for easier maintenance, reusability, and reduced material waste.

To overcome all these challenges, several strategies can be employed. Enhancing the mechanical properties of cation-alginate complexes through chemical modifications and the addition of reinforcing agents, such as fibers or fillers, can offer a major step forward in the improvement of isolation capabilities. Advanced techniques like additive manufacturing can allow the crafting of complex structures that optimize isolation by better distributing mechanical forces. Additionally, developing formulations that balance strong yet reversible adhesion can significantly contribute to the overall durability and sustainability of these materials.

5. Conclusion

The complexation of alginate with various cations represents an extremely powerful strategy for modulating the physicochemical properties of alginate-based hydrogels. Alginate, thanks to its sustainability, its ability to interact with various cations, and the resulting diverse properties, represents a unique building block for the development of hybrid materials when combined with cationic species. By fully controlling the interplay of thermodynamics and kinetics ruling the complexation process, and gaining an in-depth understanding of the supramolecular interactions between alginate and various metal cations forming functional complexes, we have explored the novel architectures and related properties that are imparted to the hybrids for each cation.

This review addresses a key gap in the literature by providing a comprehensive overview of how alginate-cation combinations influence the properties of metal-alginate complexes. We structured the content to guide research, starting with fundamental strategies and characterization techniques, particularly for less-experienced readers. We then explored ion-specific interactions at various levels, offering detailed insights into the mechanisms behind these complexes. Finally, we examined functional applications across fields like sensing and energy storage, highlighting current uses and future research directions. Each section stands alone, allowing readers to focus on areas of interest.

Opportunities and challenges toward the realization of unprecedented cation-alginate functional materials have been discussed, proposing a roadmap for future research in this dynamic field of high potential for sustainable technological breakthroughs. Their high ion-loading capacity within the polymeric matrix promotes them as active key components for advance-

ments in chemical sensors, water purification, and energy storage applications. Alginate-cation complexes also exhibit high ionic conductivity, opening the door to their application in the burgeoning field of flexible electronics, when combined with nonconductive polymers as scaffolds, to ultimately avoid the use of carbon-based fillers that can impair transparency. Tailoring matrix properties, such as thermal stability and mechanical response through careful cation selection, enhances the versatility of alginate in these applications. In the biomedical field, the ability to modify alginate's properties for specific cations enables the development of advanced drug delivery systems and tissue engineering scaffolds. By adjusting the mechanical and degradation characteristics, these formulations can be optimized for biocompatibility and functionality. The ability to finely tune these properties allows alginate to be a competitive alternative to other materials for both biomedical (tissue engineering, healing patches, artificial skins, etc.) and mechanical (mechanical isolators, reversible adhesives, etc.) applications.

Cation-alginate complexes face several overarching challenges across various applications. The high sensitivity to environmental conditions such as temperature, pH, and moisture represents a critical limitation of these materials, jeopardizing their performance and stability. This variability often impacts their effectiveness and longevity, making it crucial to address their degradation under extreme conditions, especially when used in water purification or energy storage applications. Additionally, achieving a balance between flexibility and strength remains a persistent challenge, especially when these materials are used in high mechanical stress demanding applications like artificial skin or mechanical isolators. Controlled release and specificity are other critical areas of concern. For applications like drug delivery and food supplements, the variable release rates of encapsulated cations can affect performance. This inconsistency is compounded by the challenge of ensuring selectivity in environmental and sensor applications, where precise targeting of ions or molecules is essential to ensure effectiveness. Ensuring biocompatibility and minimizing toxicity is crucial, especially for biomedical uses. The safety of cation-alginate complexes must be guaranteed to avoid adverse effects, which can be a significant barrier to their clinical implementation. Uniformity in structural and functional integrity is another key challenge. Inconsistent integration of cation-alginate complexes within materials can lead to uneven performance, which is particularly problematic in applications where reliability is crucial.

To address all these challenges, we have identified several promising future directions. Advanced processing techniques such as spray-drying, electrospinning, and additive manufacturing offer potential solutions for enhancing the consistency and performance of these complexes. By developing multication complexes, researchers aim to improve efficacy and reduce issues like resistance development. Chemical modifications and reinforcements can also play a crucial role. Enhancing the mechanical properties of alginate through chemical tweaks or incorporating reinforcing agents can significantly improve stability and performance. These modifications help ensure that the materials maintain their integrity and functionality under various conditions. Enhanced specificity and controlled release are key to improving performance in applications like sensors and drug delivery systems. Integrating selective recognition elements, such as molecularly imprinted polymers or aptamers, can increase the specificity of sensors, while advanced encapsulation methods can better control the release profiles of therapeutic agents. The integration of high-performance materials, such as graphene or carbon nanotubes, with cation-alginate complexes offers a powerful strategy to boost conductivity and performance, especially in supercapacitors and mechanical isolators. Finally, adopting eco-friendly approaches and focusing on sustainable technologies will be important for developing greener solutions in catalysis and environmental remediation. By overcoming these limitations and exploring these future directions, cation-alginate complexes would become more versatile and effective for a wide range of applications.

All in all, alginate-metal complexes have proven to be sustainable, versatile functional hybrids with on-demand properties and high potential to drive innovations in sensing, catalysis, energy storage, environmental remediation, and filtration technologies, shaping sustainable solutions for diverse disruptive applications.

Acknowledgements

The authors acknowledged financial supports from the CSGI (Consorzio Interuniversitario per lo Sviluppo dei Sistemi a Grande Interfase), the MUR-Italy ("Progetto Dipartimenti di Eccellenza 2023–2027" and "Progetto Dipartimenti di Eccellenza 2018–2022" (58503DIP_ECC) allocated to Department of Chemistry "Ugo Schiff"), the National Recovery and Resilience Plan (NRRP), Mission 4 Component 2 "Dalla ricerca all'impresa"—Call for tender No. 341 of 15/03/2022 of Italian Ministry of Research funded by the European Union – NextGenerationEU, CUP: B83C22004890007, as well as the Agence Nationale de la Recherche through the Interdisciplinary Thematic Institute SysChem via the IdEx Unistra (ANR-10-IDEX-0002) within the program Investissement d'Avenir, the Foundation Jean-Marie Lehn, and the Institut Universitaire de France (IUF).

Conflict of Interest

The authors declare no conflict of interest.

Keywords

alginate, biopolymer, functional materials, hydrogels, ionic crosslinking

Received: September 3, 2024
Revised: October 8, 2024
Published online:

[1] H. S. Yoon, R. A. Andersen, S. M. Boo, D. Bhattacharya, in *Encyclopedia of Microbiology*, 3rd ed., (Ed: M. Schaechter), Academic Press, Oxford **2009**, p. 721.
[2] E. C. C. Stanford, *British Patent* **1881**, *142*.
[3] G. Skjåk-Bræk, H. Grasdalen, B. Larsen, *Carbohydr. Res.* **1986**, *154*, 239.
[4] H. Grasdalen, B. Larsen, O. Smisrod, *Carbohydr. Res.* **1981**, *89*, 179.
[5] T. Salomonsen, H. M. Jensen, F. H. Larsen, S. Steuernagel, S. B. Engelsen, *Carbohydr. Res.* **2009**, *344*, 2014.
[6] H. Grasdalen, *Carbohydr. Res.* **1983**, *118*, 255.
[7] H. Grasdalen, B. Larsen, O. Smidsrød, *Carbohydr. Res.* **1979**, *68*, 23.

[8] O. Aarstad, B. L. Strand, L. M. Klepp-Andersen, G. Skjåk-Bræk, *Biomacromolecules* **2013**, *14*, 3409.
[9] H. Huang, B. Larsen, *Acta Chem. Scand.* **1962**, *16*, 1908.
[10] H. Haug, B. Larsen, O. Smidsrød, *Acta Chem. Scand.* **1967**, *21*, 691.
[11] K. Y. Lee, D. J. Mooney, *Prog. Polym. Sci.* **2012**, *37*, 106.
[12] C. Hu, W. Lu, A. Mata, K. Nishinari, Y. Fang, *Int. J. Biol. Macromol.* **2021**, *177*, 578.
[13] R. M. Hassan, *Polym. Int.* **1993**, *31*, 81.
[14] S. Fu, A. Thacker, D. M. Sperger, R. L. Boni, I. S. Buckner, S. Velankar, E. J. Munson, L. H. Block, *AAPS PharmSciTech* **2011**, *12*, 453.
[15] G. T. Grant, E. R. Morris, D. A. Rees, P. J. C. Smith, D. Thom, *FEBS Lett.* **1973**, *32*, 195.
[16] E. R. Morris, D. A. Rees, D. Thom, J. Boyd, *Carbohydr. Res.* **1978**, *66*, 145.
[17] H.-R. Lee, S. M. Jung, S. Yoon, W. H. Yoon, T. H. Park, S. Kim, H. W. Shin, D. S. Hwang, S. Jung, *Sci. Rep.* **2019**, *9*, 12357.
[18] M. Stewart, S. Gray, T. Vasiljevic, J. Orbell, *Carbohydr. Polym.* **2014**, *102*, 246.
[19] S. N. Pawar, K. J. Edgar, *Biomaterials* **2012**, *33*, 3279.
[20] J.-S. Yang, Y.-J. Xie, W. He, *Carbohydr. Polym.* **2011**, *84*, 33.
[21] C. C. Cutright, J. L. Harris, S. Ramesh, S. A. Khan, J. Genzer, S. Menegatti, *Adv. Funct. Mater.* **2021**, *31*, 2104164.
[22] L. Tao, C. Shi, Y. Zi, H. Zhang, X. Wang, J. Zhong, *Food Hydrocolloids* **2023**, *147*, 109338.
[23] I. Fernández Farrés, I. T. Norton, *Food Hydrocolloids* **2014**, *40*, 76.
[24] B. Amsden, N. Turner, *Biotechnol. Bioeng.* **1999**, *65*, 605.
[25] W.-P. Voo, C.-W. Ooi, A. Islam, B.-T. Tey, E.-S. Chan, *Eur. Polym. J.* **2016**, *75*, 343.
[26] F. Xie, H. Cao, L. Ma, X. Hua, C. Li, *J. Mater. Res.* **2021**, *36*, 1487.
[27] S. K. Papageorgiou, F. K. Katsaros, E. P. Kouvelos, J. W. Nolan, H. L. Deit, N. K. Kanellopoulos, *J. Hazard. Mater.* **2006**, *137*, 1765.
[28] N. Wang, B. Wang, Y. Wan, B. Gao, V. D. Rajput, *J. Environ. Manage.* **2023**, *348*, 119133.
[29] M. de Souza Gomes, M. das Graças Cardoso, A. C. G. Guimarães, A. C. Guerreiro, C. M. L. Gago, E. V. de Barros Vilas Boas, C. M. B. Dias, A. C. C. Manhita, M. L. Faleiro, M. G. C. Miguel, M. D. C. Antunes, *J. Sci. Food Agric.* **2017**, *97*, 929.
[30] A. Gupta, J. Bhasarkar, M. R. Chandan, A. H. Shaik, B. Kiran, D. K. Bal, *J. Macromol. Sci., Part B: Phys.* **2020**, *59*, 713.
[31] D. Luna-Vital, R. Cortez, P. Ongkowijoyo, E. Gonzalez de Mejia, *Food Res. Int.* **2018**, *105*, 169.
[32] X. Zhang, L. Wang, L. Weng, B. Deng, *J. Appl. Polym. Sci.* **2020**, *137*, 48571.
[33] M. Qi, Y. Mørch, I. Lacík, K. Formo, E. Marchese, Y. Wang, K. K. Danielson, K. Kinzer, S. Wang, B. Barbaro, G. Kolláriková, D. Chorvát Jr, D. Hunkeler, G. Skjåk-Bræk, J. Oberholzer, B. L. Strand, *Xenotransplantation* **2012**, *19*, 355.
[34] D. H. Camacho, S. J. Y. Uy, M. J. F. Cabrera, M. O. S. Lobregas, T. J. M. C. Fajardo, *Food Res. Int.* **2019**, *119*, 15.
[35] V. Mouriño, P. Newby, F. Pishbin, J. P. Cattalini, S. Lucangioli, A. R. Boccaccini, *Soft Matter* **2011**, *7*, 6705.
[36] I. P. S. Fernando, W. Lee, E. J. Han, G. Ahn, *Chem. Eng. J.* **2020**, *391*, 123823.
[37] A. Bibi, S. Rehman, A. Yaseen, *Mater. Res. Express* **2019**, *6*, 092001.
[38] F. Zia, H. Sobhani, M. Mohammadi, M. Athar, M. Afzal, T. Sultana, Y. Shchipunov, *Algae Based Polymers, Blends, and Composites*, Elsevier, Amsterdam **2017**, p. 603.
[39] A. K. A. Aljarid, M. Dong, Y. Hu, C. Wei, J. P. Salvage, D. G. Papageorgiou, C. S. Boland, *Adv. Funct. Mater.* **2023**, *33*, 2303837.
[40] Y. Li, G. Li, W. Li, F. Yang, H. Liu, *Nano* **2015**, *10*, 1550108.
[41] X. Chen, X. Zhao, G. Wang, *Carbohydr. Polym.* **2020**, *244*, 116311.
[42] N. Rescignano, R. Hernandez, L. D. Lopez, I. Calvillo, J. M. Kenny, C. Mijangos, *Polym. Int.* **2016**, *65*, 921.
[43] J. You, C. Zhao, J. Cao, J. Zhou, L. Zhang, *J. Mater. Chem. A* **2014**, *2*, 8491.
[44] Supriya, J. K. B., S. Sengupta, *J. Nanosci. Nanotechnol.* **2019**, *19*, 7487.
[45] L. Tarusha, S. Paoletti, A. Travan, E. Marsich, *J. Mater. Sci.: Mater. Med.* **2018**, *29*, 22.
[46] K. Neibert, V. Gopishetty, A. Grigoryev, I. Tokarev, N. Al-Hajaj, J. Vorstenbosch, A. Philip, S. Minko, D. Maysinger, *Adv. Healthcare Mater.* **2012**, *1*, 621.
[47] G. Ciofani, V. Raffa, Y. Obata, A. Menciassi, P. Dario, S. Takeoka, *Curr. Nanosci.* **2008**, *4*, 212.
[48] V. Rocher, J.-M. Siaugue, V. Cabuil, A. Bee, *Water Res.* **2008**, *42*, 1290.
[49] E. Colusso, A. Martucci, *J. Mater. Chem. C* **2021**, *9*, 5578.
[50] P. Zarrintaj, F. Seidi, M. Azarfam, M. Khodadadi, A. Erfani, M. Barani, N. P. S. Chauhan, N. Rabiee, T. Kuang, J. Kucińska-Lipka, M. Saeb, M. Mozafari, *Composites, Part B* **2023**, *258*, 110701.
[51] N. M. Iverson, P. W. Barone, M. Shandell, L. J. Trudel, S. Sen, F. Sen, V. Ivanov, E. Atolia, E. Farias, T. P. McNicholas, N. Reuel, N. M. A. Parry, G. N. Wogan, M. S. Strano, *Nat. Nanotechnol.* **2013**, *8*, 873.
[52] F. Zhuo, J. Zhou, Y. Liu, J. Xie, H. Chen, X. Wang, J. Luo, Y. Fu, A. Elmarakbi, H. Duan, *Adv. Funct. Mater.* **2023**, *33*, 2308487.
[53] Z. Zhou, J. Liu, X. Zhang, D. Tian, Z. Zhan, C. Lu, *Adv. Mater. Interfaces* **2019**, *6*, 1802040.
[54] B. Wicklein, G. Valurouthu, H. Yoon, H. Yoo, S. Ponnan, M. Mahato, J. Kim, S. S. Ali, J. Y. Park, Y. Gogotsi, I.-K. Oh, *ACS Appl. Mater. Interfaces* **2024**, *16*, 23948.
[55] J. Wang, Z. Zhang, J. Zhu, M. Tian, S. Zheng, F. Wang, X. Wang, L. Wang, *Nat. Commun.* **2020**, *11*, 3540.
[56] H. Zhi, P. Yan, D. Wang, Y. Liu, J. Tang, X. Yang, Z. Liu, Y. Zhang, N. Li, M. An, H. Liu, G. Xue, *Adv. Funct. Mater.* **2024**, *34*, 2401922.
[57] Y. Yang, H. Hua, Z. Lv, M. Zhang, C. Liu, Z. Wen, H. Xie, W. He, J. Zhao, C. C. Li, *Adv. Funct. Mater.* **2023**, *33*, 2212446.
[58] P. Rastogi, B. Kandasubramanian, *Biofabrication* **2019**, *11*, 042001.
[59] B. Marcos, P. Gou, J. Arnau, J. Comaposada, *LWT* **2016**, *74*, 271.
[60] J. Tritz, R. Rahouadj, N. de Isla, N. Charif, A. Pinzano, D. Mainard, D. Bensoussan, P. Netter, J.-F. Stoltz, N. Benkirane-Jessel, C. Huselstein, *Soft Matter* **2010**, *6*, 5165.
[61] R. Dittrich, G. Tomandl, F. Despang, A. Bernhardt, T. Hanke, W. Pompe, M. Gelinsky, *J. Am. Ceram. Soc.* **2007**, *90*, 1703.
[62] C. A. Bonino, M. D. Krebs, C. D. Saquing, S. I. Jeong, K. L. Shearer, E. Alsberg, S. A. Khan, *Carbohydr. Polym.* **2011**, *85*, 111.
[63] J. Brus, M. Urbanova, J. Czernek, M. Pavelkova, K. Kubova, J. Vyslouzil, S. Abbrent, R. Konefal, J. Horský, D. Vetchy, J. Vysloužil, P. Kulich, *Biomacromolecules* **2017**, *18*, 2478.
[64] S. K. Papageorgiou, E. P. Kouvelos, E. P. Favvas, A. A. Sapalidis, G. E. Romanos, F. K. Katsaros, *Carbohydr. Res.* **2010**, *345*, 469.
[65] H. Zheng, J. Yang, S. Han, *J. Appl. Polym. Sci.* **2016**, *133*, https://doi.org/10.1002/app.43616.
[66] A. Forgács, V. Papp, G. Paul, L. Marchese, A. Len, Z. Dudás, I. Fábián, P. Gurikov, J. Kalmár, *ACS Appl. Mater. Interfaces* **2021**, *13*, 2997.
[67] B. T. Stokke, K. I. Draget, O. Smidsrød, Y. Yuguchi, H. Urakawa, K. Kajiwara, *Macromolecules* **2000**, *33*, 1853.
[68] Z.-Y. Wang, J. W. White, M. Konno, S. Saito, T. Nozawa, *Biopolymers* **1995**, *35*, 227.
[69] X. Zhang, X. Lin, H. Ding, Y. He, H. Yang, Y. Chen, X. Chen, X. Luo, *Ecotoxicol. Environ. Saf.* **2019**, *169*, 392.
[70] H. Zimmermann, M. Hillgärtner, B. Manz, P. Feilen, F. Brunnenmeier, U. Leinfelder, M. Weber, H. Cramer, S. Schneider, C. Hendrich, F. Volke, U. Zimmermann, *Biomaterials* **2003**, *24*, 2083.
[71] A. A. Solbu, A. Koernig, J. S. Kjesbu, D. Zaytseva-Zotova, M. Sletmoen, B. Strand, *Carbohydr. Polym.* **2021**, https://doi.org/10.1016/j.carbpol.2021.118804.

[72] P. Agulhon, M. Robitzer, J.-P. Habas, F. Quignard, *Carbohydr. Polym.* **2014**, *112*, 525.
[73] J. L. Drury, R. G. Dennis, D. J. Mooney, *Biomaterials* **2004**, *25*, 3187.
[74] M. C. Straccia, G. G. d'Ayala, I. Romano, P. Laurienzo, *Carbohydr. Polym.* **2015**, *125*, 103.
[75] L. Shunli, M. Kang, I. Hussain, K. Li, F. Yao, G. Fu, *Polym. Degrad. Stab.* **2016**, *133*, https://doi.org/10.1016/j.polymdegradstab.2016.07.022.
[76] P. Tordi, A. Tamayo, Y. Jeong, M. Bonini, P. Samorì, *Adv. Funct. Mater.* **2024**, 2410663, https://doi.org/10.1002/adfm.202410663.
[77] P. Tordi, R. Gelli, F. Ridi, M. Bonini, *Carbohydr. Polym.* **2024**, *326*, 121586.
[78] P. Tordi, F. Ridi, M. Bonini, *Colloids Surf., A* **2023**, *677*, 132396.
[79] Y. Liu, J. Wang, J. Zhao, C. Zhang, J. Ran, P. Zhu, *Nanomater. Energy* **2014**, *3*, 3.
[80] Y. Liu, X.-R. Zhao, Y.-L. Peng, D. Wang, L. Yang, H. Peng, P. Zhu, D.-Y. Wang, *Polym. Degrad. Stab.* **2016**, *127*, 20.
[81] Y. Liu, J.-C. Zhao, C.-J. Zhang, Y. Guo, P. Zhu, D.-Y. Wang, *J. Mater. Sci.* **2016**, *51*, https://doi.org/10.1007/s10853-015-9435-9.
[82] Y. Qin, *Polym. Adv. Technol.* **2008**, *19*, 6.
[83] S. K. Bajpai, S. Sharma, *React. Funct. Polym.* **2004**, *59*, 129.
[84] K. H. Bouhadir, K. Y. Lee, E. Alsberg, K. L. Damm, K. W. Anderson, D. J. Mooney, *Biotechnol. Prog.* **2001**, *17*, 945.
[85] M. Ghadiri, W. Chrzanowski, W. H. Lee, A. Fathi, F. Dehghani, R. Rohanizadeh, *Appl. Clay Sci.* **2013**, *85*, 64.
[86] M. Stevens, H. Qanadilo, R. Langer, V. P. Shastri, *Biomaterials* **2004**, *25*, 887.
[87] S. P. M. Bohari, D. W. L. Hukins, L. M. Grover, *Bio-Med. Mater. Eng.* **2011**, *21*, 159.
[88] D. Li, Z. Wei, C. Xue, *Compr. Rev. Food Sci. Food Saf.* **2021**, *20*, 5345.
[89] Y. Ohm, J. Liao, Y. Luo, M. J. Ford, C. Majidi, *Adv. Mater.* **2023**, *35*, 2209408.
[90] R. D. Shannon, *Acta Crystallogr., Sect. A: Cryst. Phys., Diffr., Theor. Gen. Crystallogr.* **1976**, *32*, 751.
[91] R. Hassan, *Colloids Surf.* **1991**, *60*, 203.
[92] K. Chen, F. Wang, S. Liu, X. Wu, L. Xu, D. Zhang, *Int. J. Biol. Macromol.* **2020**, *148*, 501.
[93] E. Lengert, M. Saveleva, A. Abalymov, V. Atkin, P. C. Wuytens, R. Kamyshinsky, A. L. Vasiliev, D. A. Gorin, G. B. Sukhorukov, A. G. Skirtach, B. Parakhonskiy, *ACS Appl. Mater. Interfaces* **2017**, *9*, 21949.
[94] Y. Qin, *Int. Wound J.* **2005**, *2*, 172.
[95] Y. Qin, *Polym. Int.* **2008**, *57*, 171.
[96] K. Nakamoto, *Infrared and Raman Spectra of Inorganic and Coordination Compounds*, Wiley Interscience, New York **1986**, p. 231.
[97] A. Haug, *Acta Chem. Scand.* **1961**, *15*, 1794.
[98] A. Haug, O. Smidsrød, B. Högdahl, H. A. Øye, S. E. Rasmussen, E. Sunde, N. A. Sørensen, *Acta Chem. Scand.* **1970**, *24*, 843.
[99] G. R. Seely, R. L. Hart, *Macromolecules* **1974**, *7*, 706.
[100] R. G. Schweiger, *Kolloid-Z. Z. Polym.* **1964**, *196*, 47.
[101] C. Ouwerx, N. Velings, M. M. Mestdagh, M. A. V. Axelos, *Polym. Gels Networks* **1998**, *6*, 393.
[102] R. Wang, D. Liang, X. Liu, W. Fan, S. Meng, W. Cai, *Chem. Eng. J.* **2020**, *379*, 122351.
[103] F. Topuz, A. Henke, W. Richtering, J. Groll, *Soft Matter* **2012**, *8*, 4877.
[104] M. E. Baldassarre, A. Di Mauro, M. C. Pignatelli, M. Fanelli, S. Salvatore, G. Di Nardo, A. Chiaro, L. Pensabene, N. Laforgia, *Int. J. Environ. Res. Public Health* **2019**, *17*, 83.
[105] H. Park, K. Park, W. S. W. Shalaby, *Biodegradable Hydrogels for Drug Delivery*, CRC Press, Boca Raton, FL **1993**, p. 99.
[106] O. Smidsrød, *Faraday Discuss. Chem. Soc.* **1974**, *57*, 263.
[107] H. Hecht, S. Srebnik, *Biomacromolecules* **2016**, *17*, 2160.
[108] A. A. Badwan, A. Abumalooh, E. Sallam, A. Abukalaf, O. Jawan, *Drug Dev. Ind. Pharm.* **1985**, *11*, 239.
[109] L. Segale, L. Giovannelli, P. Mannina, F. Pattarino, *Scientifica* **2016**, *2016*, 5062706.
[110] P. Khazaeli, A. Pardakhty, H. Fereshteh, *Iran. J. Pharm. Res.* **2008**, *7*, 163.
[111] B.-B. Lee, P. Ravindra, E.-S. Chan, *Chem. Eng. Technol.* **2013**, *36*, 1627.
[112] P. Hart, G. Colson, J. Burris, *J. Sci. Technol. For. Prod. Processes* **2012**, *1*, 67.
[113] D. Poncelet, V. Babak, C. Dulieu, A. Picot, *Colloids Surf., A* **1999**, *155*, 171.
[114] C. Zhang, R. A. Grossier, L. Lacaria, F. Rico, N. A. Candoni, S. A. Veesler, *Chem. Eng. Sci.* **2020**, *211*, 115322.
[115] Y. N. Mata, M. L. Blázquez, A. Ballester, F. González, J. A. Muñoz, *J. Hazard Mater.* **2009**, *163*, 555.
[116] X. Tao, S. Wang, Z. Li, S. Zhou, *Mater. Chem. Phys.* **2021**, *258*, 123931.
[117] K. T. Paige, L. G. Cima, M. J. Yaremchuk, B. L. Schloo, J. P. Vacanti, C. A. Vacanti, *Plast. Reconstr. Surg.* **1996**, *97*, 168.
[118] D. E. Weber, M. T. Semaan, J. K. Wasman, R. Beane, L. J. Bonassar, C. A. Megerian, *Laryngoscope* **2006**, *116*, 700.
[119] T. A. Becker, D. R. Kipke, T. Brandon, *J. Biomed. Mater. Res.* **2001**, *54*, 76.
[120] Z. Chen, J. Song, Y. Xia, Y. Jiang, L. L. Murillo, O. Tsigkou, T. Wang, Y. Li, *Mater. Sci. Eng., C* **2021**, *127*, 112204.
[121] G. K. Xu, L. Liu, J. M. Yao, *Adv. Mater. Res.* **2013**, *796*, 87.
[122] D. Ji, J. M. Park, M. S. Oh, T. L. Nguyen, H. Shin, J. S. Kim, D. Kim, H. S. Park, J. Kim, *Nat. Commun.* **2022**, *13*, 3019.
[123] P. dos Santos Araújo, G. B. Belini, G. P. Mambrini, F. M. Yamaji, W. R. Waldman, *Int. J. Biol. Macromol.* **2019**, *140*, 749.
[124] N. Patel, D. Lalwani, S. Gollmer, E. Injeti, Y. Sari, J. Nesamony, *Prog. Biomater.* **2016**, *5*, 117.
[125] J. Guo, X. Liu, N. Jiang, A. K. Yetisen, H. Yuk, C. Yang, A. Khademhosseini, X. Zhao, S.-H. Yun, *Adv. Mater.* **2016**, *28*, 10244.
[126] R. Tong, Z. Ma, R. Yao, P. Gu, T. Li, L. Liu, F. Guo, M. Zeng, J. Xu, *Int. J. Biol. Macromol.* **2023**, *246*, 125667.
[127] X. Zhang, K. Wang, J. Hu, Y. Zhang, Y. Dai, F. Xia, *J. Mater. Chem. A* **2020**, *8*, 25390.
[128] A. Li, T. Gong, Y. Hou, X. Yang, Y. Guo, *Int. J. Biol. Macromol.* **2020**, *146*, 821.
[129] N. Nourmohammadi, S. Soleimanian-Zad, H. Shekarchizadeh, *J. Sci. Food Agric.* **2020**, *100*, 5260.
[130] A. C. K. Bierhalz, M. A. da Silva, T. G. Kieckbusch, *J. Food Eng.* **2012**, *110*, 18.
[131] Z. Deng, F. Wang, B. Zhou, J. Li, B. Li, H. Liang, *Food Hydrocolloids* **2019**, *89*, 691.
[132] P. Agulhon, V. Markova, M. Robitzer, F. Quignard, T. Mineva, *Biomacromolecules* **2012**, *13*, 1899.
[133] R. Pastore, C. Siviello, F. Greco, D. Larobina, *Macromolecules* **2020**, *53*, 649.
[134] O. Catanzano, A. Soriente, A. La Gatta, M. Cammarota, G. Ricci, I. Fasolino, C. Schiraldi, L. Ambrosio, M. Malinconico, P. Laurienzo, M. G. Raucci, G. Gomez d'Ayala, *Carbohydr. Polym.* **2018**, *202*, 72.
[135] E. S. Place, L. Rojo, E. Gentleman, J. P. Sardinha, M. M. Stevens, *Tissue Eng., Part A* **2011**, *17*, 2713.
[136] A. Hassani, Ç. B. Avci, S. N. Kerdar, H. Amini, M. Amini, M. Ahmadi, S. Sakai, B. G. Bagca, N. P. Ozates, R. Rahbarghazi, A. B. Khoshfetrat, *J. Nanobiotechnol.* **2022**, *20*, 310.
[137] N. Yuan, L. Jia, Z. Geng, R. Wang, Z. Li, X. Yang, Z. Cui, S. Zhu, Y. Liang, Y. Liu, *BioMed. Res. Int.* **2017**, *2017*, 9867819.
[138] Y. Zhang, H. Li, H. Xu, L. Wang, M. Zhang, J. Liu, F. Tan, *J. Mater. Sci.* **2021**, *56*, 17221.
[139] A. Henriques Lourenço, N. Neves, C. Ribeiro-Machado, S. R. Sousa, M. Lamghari, C. C. Barrias, A. Trigo Cabral, M. A. Barbosa, C. C. Ribeiro, *Sci. Rep.* **2017**, *7*, 5098.

[140] A. Moreiraa, M. Sader, G. Soaresb, M. H. Rocha-Leão, *Mater. Res.* **2014**, *17*, 967.
[141] N. Neves, B. B. Campos, I. F. Almeida, P. C. Costa, A. T. Cabral, M. A. Barbosa, C. C. Ribeiro, *Mater. Sci. Eng., C* **2016**, *59*, 818.
[142] Y. A. Mørch, I. Donati, B. L. Strand, G. Skjåk-Braek, *Biomacromolecules* **2006**, *7*, 1471.
[143] S.-L. Huang, Y.-S. Lin, *Adv. Mater. Sci. Eng.* **2017**, *2017*, 9304592.
[144] Y. Liu, C.-J. Zhang, J.-C. Zhao, Y. Guo, P. Zhu, D.-Y. Wang, *Carbohydr. Polym.* **2016**, *139*, 106.
[145] M. S. Shoichet, R. H. Li, M. L. White, S. R. Winn, *Biotechnol. Bioeng.* **1996**, *50*, 374.
[146] X. P. Bai, H. X. Zheng, R. Fang, T. R. Wang, X. L. Hou, Y. Li, X. B. Chen, W. M. Tian, *Biomed. Mater.* **2011**, *6*, 045002.
[147] V. F. Duvivier-Kali, A. Omer, R. J. Parent, J. J. O'Neil, G. C. Weir, *Diabetes* **2001**, *50*, 1698.
[148] T. Zekorn, A. Horcher, U. Siebers, R. Schnettler, G. Klöck, B. Hering, U. Zimmermann, R. G. Bretzel, K. Federlin, *Acta Diabetol.* **1992**, *29*, 99.
[149] S. Uzaşçı, F. Tezcan, F. B. Erim, *Int. J. Environ. Sci. Technol.* **2014**, *11*, 1861.
[150] L. Xu, K. Chen, G. Q. Chen, S. E. Kentish, G. Kevin Li, *Front. Chem. Sci. Eng.* **2021**, *15*, 198.
[151] Y. Zhang, K. Zhao, Z. Yang, Z. Zhang, Z. Guo, R. Chu, W. Zhang, W. Shi, J. Li, Z. Li, H. Liu, A. Xu, X. Chen, *Sep. Purif. Technol.* **2021**, *270*, 118761.
[152] M. A. Shannon, P. W. Bohn, M. Elimelech, J. G. Georgiadis, B. J. Mariñas, A. M. Mayes, *Nature* **2008**, *452*, 301.
[153] N. Emmerichs, J. Wingender, H.-C. Flemming, C. Mayer, *Int. J. Biol. Macromol.* **2004**, *34*, 73.
[154] J.-P. Habas, E. Pavie, A. Lapp, J. Peyrelasse, *J. Rheol.* **2004**, *48*, 1.
[155] IUPAC. Compendium of Chemical Terminology, 3rd ed. *(the "Gold Book")*, Compiled by A. D. McNaught, A. Wilkinson, Blackwell Scientific Publications, Oxford, (2019-) (Eds. S. J. Chalk), **1997**, https://doi.org/10.1351/goldbook.G02600.
[156] Ý. A. Mørch, I. Sandvig, Ø. Olsen, I. Donati, M. Thuen, G. Skjåk-Bræk, O. Haraldseth, C. Brekken, *Contrast Media Mol. Imaging* **2012**, *7*, 265.
[157] L. Kalkowski, D. Golubczyk, J. Kwiatkowska, P. Holak, K. Milewska, M. Janowski, J. M. Oliveira, P. Walczak, I. Malysz-Cymborska, *Pharmaceutics* **2021**, *13*, 1076.
[158] M. Su, Y. Zhu, J. Chen, B. Zhang, C. Sun, M. Chen, X. Yang, *Chem. Eng. J.* **2022**, *435*, 134926.
[159] P. L.-B. Cheton, F. S. Archibald, *Free Radical Biol. Med.* **1988**, *5*, 325.
[160] W. Mao, L. Zhang, Y. Zhang, Y. Wang, N. Wen, Y. Guan, *Chemosphere* **2022**, *292*, 133391.
[161] W. Mao, L. Zhang, Y. Zhang, Y. Guan, *Environ. Sci.: Nano* **2022**, *9*, 214.
[162] L. Leyssens, B. Vinck, C. Van Der Straeten, F. Wuyts, L. Maes, *Toxicology* **2017**, *387*, 43.
[163] B. Orhan, T. R. Adetoro, H. Kaygusuz, *ChemRxiv* **2022**, https://doi.org/10.26434/chemrxiv-2022-x8k4d.
[164] D. Das, B. J. Saikia, *Chem. Phys. Impact* **2023**, *6*, 100137.
[165] S. Focaroli, G. Teti, V. Salvatore, I. Orienti, M. Falconi, *Stem Cells Int.* **2016**, *2016*, e2030478.
[166] C. Liu, Y. Tao, Y.-J. Xu, Y. Liu, P. Zhu, Y.-Z. Wang, *Macromol. Mater. Eng.* **2021**, *306*, 2100466.
[167] G. Genchi, A. Carocci, G. Lauria, M. S. Sinicropi, A. Catalano, *Int. J. Environ. Res. Public Health* **2020**, *17*, 679.
[168] R. Hassan, M. H. Wahdan, A. Hassan, *Eur. Polym. J.* **1988**, *24*, 281.
[169] Y. Liu, J.-C. Zhao, C.-J. Zhang, Y. Guo, L. Cui, P. Zhu, D.-Y. Wang, *RSC Adv.* **2015**, *5*, 64125.
[170] Y. Abdellaoui, C. A. Celaya, M. Elhoudi, R. Boualou, H. Agalit, M. Reina, P. Gamero-Melo, H. A. Oualid, *J. Mol. Struct.* **2022**, *1249*, 131524.
[171] Z. Xiong, L. Sun, H. Yang, Z. Xiao, Z. Deng, Q. Li, C. Wang, F. Shen, Z. Liu, *Adv. Funct. Mater.* **2023**, *33*, 2211423.
[172] A.-M. Dumitrașcu, I. Caraș, C. Țucureanu, A.-L. Ermeneanu, V.-C. Tofan, *Gels* **2022**, *8*, 66.
[173] Z. Wang, G. M. Kale, M. Ghadiri, *J. Am. Ceram. Soc.* **2012**, *95*, 3124.
[174] N. M. Sami, A. A. Elsayed, M. M. S. Ali, S. S. Metwally, *Environ. Sci. Pollut. Res.* **2022**, https://doi.org/10.1007/s11356-022-21305-8.
[175] J. Rodrigues, R. Lagoa, *J. Carbohydr. Chem.* **2006**, *25*, 219.
[176] H. Zheng, *Carbohydr. Res.* **1997**, *302*, 97.
[177] N. S. Heliopoulos, S. K. Papageorgiou, A. Galeou, E. P. Favvas, F. K. Katsaros, K. Stamatakis, *Surf. Coat. Technol.* **2013**, *235*, 24.
[178] M. Grace, N. Chand, S. K. Bajpai, *J. Eng. Fibers Fabr.* **2009**, *4*, 155892500900400303.
[179] J. Qi, Z. Zheng, L. Hu, H. Wang, B. Tang, L. Lin, *Colloids Surf., B* **2022**, *212*, 112339.
[180] W. Klinkajon, P. Supaphol, *Biomed. Mater.* **2014**, *9*, 045008.
[181] S. Wang, X. Liu, M. Lei, J. Sun, X. Qu, C. Liu, *J. Mater. Sci.: Mater. Med.* **2021**, *32*, 143.
[182] K. Rajender Reddy, K. Rajgopal, M. Lakshmi Kantam, *Catal. Lett.* **2007**, *114*, 36.
[183] L. Bahsis, E.-H. Ablouh, H. Anane, M. Taourirte, M. Julve, S.-E. Stiriba, *RSC Adv.* **2020**, *10*, 32821.
[184] J. F. Souza, T. F. B. de Aquino, J. E. R. Nascimento, R. G. Jacob, A. R. Fajardo, *Catal. Sci. Technol.* **2020**, *10*, 3918.
[185] Z. Zhang, T. Lin, S. Li, X. Chen, X. Que, L. Sheng, Y. Hu, J. Peng, H. Ma, J. Li, W. Zhang, M. Zhai, *Macromol. Biosci.* **2022**, *22*, 2100361.
[186] J. S. Rowbotham, P. W. Dyer, H. C. Greenwell, D. Selby, M. K. Theodorou, *Interface Focus* **2013**, *3*, 20120046.
[187] L. Chan, Y. Jin, P. Heng, *Int. J. Pharm.* **2002**, *242*, 255.
[188] S. Pistone, D. Qoragllu, G. Smistad, M. Hiorth, *Soft Matter* **2015**, *11*, 5765.
[189] R. J. Miller, A. S. Adeleye, H. M. Page, L. Kui, H. S. Lenihan, A. A. Keller, *J. Nanopart. Res.* **2020**, *22*, 129.
[190] H. Rabiee, V. Vatanpour, M. H. D. A. Farahani, H. Zarrabi, *Sep. Purif. Technol.* **2015**, *156*, 299.
[191] L. Abi Nassif, S. Rioual, W. Farah, M. Fauchon, Y. Toueix, C. Hellio, M. Abboud, B. Lescop, *J. Environ. Chem. Eng.* **2020**, *8*, 104246.
[192] F. Zhong, C. Chen, J. Zheng, L. Li, X. Wen, *Colloids Surf., A* **2022**, *647*, 129200.
[193] C. Peretiatko, E. Hupalo, J. Campos, C. Budziak-Parabocz, *Orbital: Electron. J. Chem.* **2018**, *10*, https://dx.doi.org/10.17807/orbital.v10i3.1103.
[194] X. Wen, K. Jiang, H. Zhang, H. Huang, L. Yang, Z. Zhou, Q. Weng, *Materials* **2022**, *15*, 1767.
[195] Q. Liu, Y. Wang, X. Hong, R. Zhou, Z. Hou, B. Zhang, *Adv. Energy Mater.* **2022**, *12*, 2200318.
[196] C. J. Gray, J. Dowsett, *Biotechnol. Bioeng.* **1988**, *31*, 607.
[197] G. Genchi, M. S. Sinicropi, G. Lauria, A. Carocci, A. Catalano, *Int. J. Environ. Res. Public Health* **2020**, *17*, 3782.
[198] T. A. Davis, M. Ramirez, A. Mucci, B. Larsen, *J. Appl. Phycol.* **2004**, *16*, 275.
[199] Z. Wang, S. Wu, Y. Zhang, L. Miao, Y. Zhang, A. Wu, *Int. J. Biol. Macromol.* **2020**, *157*, 687.
[200] S. Cataldo, G. Cavallaro, A. Gianguzza, G. Lazzara, A. Pettignano, D. Piazzese, I. Villaescusa, *J. Environ. Chem. Eng.* **2013**, *1*, 1252.
[201] I. Cosme-Torres, M. G. Macedo-Miranda, P. Ibarra-Escutia, M. Manjarrez-Olvera, V. Albíter-López, A. Trujillo-Segura, *MRS Adv.* **2020**, *5*, 3247.
[202] Z. Wang, N. Liu, F. Feng, Z. Ma, *Biosens. Bioelectron.* **2015**, *70*, 98.
[203] C. Lamelas, F. Avaltroni, M. Benedetti, K. J. Wilkinson, V. I. Slaveykova, *Biomacromolecules* **2005**, *6*, 2756.

[204] I.-L. Andresen, O. Smidsørod, *Carbohydr. Res.* **1977**, *58*, 271.
[205] A. L. Wani, A. Ara, J. A. Usmani, *Interdiscip. Toxicol.* **2015**, *8*, 55.
[206] D. Tahtat, M. N. Bouaicha, S. Benamer, A. Nacer-Khodja, M. Mahlous, *Int. J. Biol. Macromol.* **2017**, *105*, 1010.
[207] S. Cataldo, A. Gianguzza, M. Merli, N. Muratore, D. Piazzese, M. L. Turco Liveri, *J. Colloid Interface Sci.* **2014**, *434*, 77.
[208] R. M. Hassan, Y. Ikeda, H. Tomiyasu, *J. Mater. Sci.* **1993**, *28*, 5143.
[209] I. Zaafarany, K. Khairou, R. Hassan, *High Perform. Polym.* **2010**, *22*, 69.
[210] I. Zaafarany, *J. King Abdulaziz Univ., Sci.* **2010**, *22*, 193.
[211] Z. Milin, L. Wenbin, G. Xuguo, Preparation method of chromium alginate Patent CN1443781A, **2003**, https://patents.google.com/patent/CN1443781A/en?oq=CN1443781A.
[212] M. M. Araújo, J. A. Teixeira, *Int. Biodeterior. Biodegrad.* **1997**, *40*, 63.
[213] K. J. Sreeram, H. Yamini Shrivastava, B. U. Nair, *Biochim. Biophys. Acta, Gen. Subj.* **2004**, *1670*, 121.
[214] *Studies in Environmental Science* (Ed: S. E. Jørgensen), Elsevier, Amsterdam **1979**, pp. 309–313.
[215] P. Singh, S. K. Singh, J. Bajpai, A. K. Bajpai, R. B. Shrivastava, *J. Mater. Res. Technol.* **2014**, *3*, 195.
[216] T. K. Das, Q. Scott, A. N. Bezbaruah, *Chemosphere* **2021**, *281*, 130837.
[217] J. Wu, H. Zheng, F. Zhang, R. J. Zeng, B. Xing, *Chem. Eng. J.* **2019**, *362*, 21.
[218] W. Zhang, F. Liu, Y. Sun, J. Zhang, Z. Hao, *Appl. Catal., B* **2019**, *259*, 118046.
[219] R. F. N. Quadrado, A. R. Fajardo, *Carbohydr. Polym.* **2017**, *177*, 443.
[220] G. Li, T. Gao, G. Fan, Z. Liu, Z. Liu, J. Jiang, Y. Zhao, *ACS Appl. Mater. Interfaces* **2020**, *12*, 6407.
[221] R. P. Narayanan, G. Melman, N. J. Letourneau, N. L. Mendelson, A. Melman, *Biomacromolecules* **2012**, *13*, 2465.
[222] I. Machida-Sano, Y. Matsuda, H. Namiki, *Biomed. Mater.* **2009**, *4*, 025008.
[223] I. Machida-Sano, S. Ogawa, H. Ueda, Y. Kimura, N. Satoh, H. Namiki, *Int. J. Biomater.* **2012**, *2012*, 1.
[224] V. Privman, S. Domanskyi, R. A. S. Luz, N. Guz, M. L. Glasser, E. Katz, *ChemPhysChem* **2016**, *17*, 976.
[225] Z. Jin, A. M. Harvey, S. Mailloux, J. Halámek, V. Bocharova, M. R. Twiss, E. Katz, *J. Mater. Chem.* **2012**, *22*, 19523.
[226] Z. Jin, G. Güven, V. Bocharova, J. Halámek, I. Tokarev, S. Minko, A. Melman, D. Mandler, E. Katz, *ACS Appl. Mater. Interfaces* **2012**, *4*, 466.
[227] H. Kaygusuz, M. H. Çoşkunırmak, N. Kahya, F. B. Erim, *Water Air Soil Pollut.* **2014**, *226*, 2257.
[228] Q. Zhou, X. Lin, B. Li, X. Luo, *Chem. Eng. J.* **2014**, *256*, 306.
[229] R. Al-Otoum, S. R. Abulateefeh, M. O. Taha, *Pharmazie* **2014**, *69*, 10.
[230] K. Venkata, M. Nagabhushanam, *Asian J. Pharm. Clin. Res.* **2019**, *12*, 246.
[231] Y. Liu, Z. Li, J. Wang, P. Zhu, J. Zhao, C. Zhang, Y. Guo, X. Jin, *Polym. Degrad. Stab.* **2015**, *118*, 59.
[232] C. H. Yang, M. X. Wang, H. Haider, J. H. Yang, J.-Y. Sun, Y. M. Chen, J. Zhou, Z. Suo, *ACS Appl. Mater. Interfaces* **2013**, *5*, 10418.
[233] X. Li, M. Li, L. Zong, X. Wu, J. You, P. Du, C. Li, *Adv. Funct. Mater.* **2018**, *28*, 1804197.
[234] C. R. Chitambar, *Biochim. Biophys. Acta, Mol. Cell Res.* **2016**, *1863*, 2044.
[235] H. Rastin, M. Ramezanpour, K. Hassan, A. Mazinani, T. T. Tung, S. Vreugde, D. Losic, *Carbohydr. Polym.* **2021**, *264*, 117989.
[236] V. Mouriño, P. Newby, A. R. Boccaccini, *Adv. Eng. Mater.* **2010**, *12*, B283.
[237] M. Khotimchenko, V. Kovalev, E. Khozhaenko, R. Khotimchenko, *Int. J. Environ. Sci. Technol.* **2015**, *12*, 3107.
[238] B. Li, C. Chen, *J. Dispersion Sci. Technol.* **2021**, *43*, 2142.
[239] J. He, A. Cui, F. Ni, S. Deng, F. Shen, G. Yang, *J. Colloid Interface Sci.* **2018**, *531*, 37.
[240] B. Li, H. Yin, *J. Polym. Environ.* **2020**, *28*, 2137.
[241] F. H. Firsching, J. C. Kell, *J. Chem. Eng. Data* **1993**, *38*, 132.
[242] B. Wang, W. Zhang, L. Li, W. Guo, J. Xing, H. Wang, X. Hu, W. Lyu, R. Chen, J. Song, L. Chen, Z. Hong, *Chemosphere* **2020**, *256*, 127124.
[243] L. Feng, Q. Zhang, F. Ji, L. Jiang, C. Liu, Q. Shen, Q. Liu, *Chem. Eng. J.* **2022**, *430*, 132754.
[244] S. Liu, F. Fan, Z. Ni, J. Liu, S. Wang, *J. Cleaner Prod.* **2023**, *385*, 135649.
[245] J. M. Huggett, *Reference Module in Earth Systems and Environmental Sciences*, Elsevier, Amsterdam **2015**.
[246] B. Li, H. Yin, *J. Dispersion Sci. Technol.* **2020**, *42*, 1.
[247] M. Elhoudi, R. Oukhrib, C. A. Celaya, D. G. Araiza, Y. Abdellaoui, I. Barra, Y. Brahmi, H. Bourzi, M. Reina, A. Albourine, H. A. Oualid, *J. Mol. Model.* **2022**, *28*, 37.
[248] B. D. Silva, A. Bastos, J. Tedim, M. Ferreira, C. Marino, I. Riegel-Vidotti, *J. Braz. Chem. Soc.* **2022**, https://doi.org/10.21577/0103-5053.20220065.
[249] Y. Wei, L. Wang, J. Wang, *Colloids Surf., A* **2022**, *636*, 128161.
[250] T. Ma, X. Zhai, Y. Huang, M. Zhang, P. Li, Y. Du, *J. Rare Earths* **2022**, *40*, 1407.
[251] U. Rocha, K. U. Kumar, C. Jacinto, I. Villa, F. Sanz-Rodríguez, M. del Carmen Iglesias de la Cruz, A. Juarranz, E. Carrasco, F. C. J. M. van Veggel, E. Bovero, J. G. Solé, D. Jaque, *Small* **2014**, *10*, 1141.
[252] Q. Huang, S. Liu, K. Li, I. Hussain, F. Yao, G. Fu, *J. Mater. Sci. Nanotechnol.* **2017**, *33*, 821.
[253] Y. Konishi, S. Asai, J. Shimaoka, M. Miyata, T. Kawamura, *Ind. Eng. Chem. Res.* **1992**, *31*, 2303.
[254] Q. Ma, Q. Wang, *Carbohydr. Polym.* **2015**, *133*, 19.
[255] K. Podgórna, K. Szczepanowicz, M. Piotrowski, M. Gajdošová, F. Štěpánek, P. Warszyński, *Colloids Surf., B* **2017**, *153*, 183.
[256] X. Li, Y. Qi, Y. Li, Y. Zhang, X. He, Y. Wang, *Bioresour. Technol.* **2013**, *142*, 611.
[257] Z. Qing, L. Wang, X. Liu, Z. Song, F. Qian, Y. Song, *Chemosphere* **2022**, *291*, 133103.
[258] S. Shan, H. Tang, Y. Zhao, W. Wang, F. Cui, *Chem. Eng. J.* **2019**, *359*, 779.
[259] I. Aswin Kumar, N. Viswanathan, *Arabian J. Chem.* **2020**, *13*, 4111.
[260] B. Chen, Y. Li, Q. Du, X. Pi, Y. Wang, Y. Sun, Y. Zhang, K. Chen, M. Wang, *Mater. Today Commun.* **2022**, *32*, 104004.
[261] I. A. Zaafarany, K. S. Khairou, R. M. Hassan, Y. Ikeda, *Arabian J. Chem.* **2009**, *2*, 1.
[262] H. Ding, X. Luo, X. Zhang, H. Yang, *Colloids Surf., A* **2019**, *562*, 186.
[263] J. Libich, J. Máca, J. Vondrák, O. Čech, M. Sedlaříková, *J. Energy Storage* **2018**, *17*, 224.
[264] X. Yin, Y. Zhou, Y. Tang, D. Kong, W. Xiao, L. Gan, J. Huang, Y. Zhang, *Int. J. Biol. Macromol.* **2024**, *275*, 133252.
[265] N. Duong, A. Uthairatanakij, N. Laohakunjit, P. Jitareerat, N. Kaisangsri, *Food Biosci.* **2023**, *52*, 102410.
[266] W. Park, J.-S. Lee, G. Gao, B. S. Kim, D.-W. Cho, *Nat. Commun.* **2023**, *14*, 7696.
[267] B. A. Nerger, S. Sinha, N. N. Lee, M. Cheriyan, P. Bertsch, C. P. Johnson, L. Mahadevan, J. V. Bonventre, D. J. Mooney, *Adv. Mater.* **2024**, *36*, 2308325.
[268] Y. Zhang, C. Zhou, B. Tian, J. Xu, X. Wang, H. Dai, H. Wang, F. Xu, C. Wang, *Sci. Adv.* **2024**, *10*, eadp3654.
[269] H. Sheng, L. Jiang, Q. Wang, Z. Zhang, Y. Lv, H. Ma, H. Bi, J. Yuan, M. Shao, F. Li, W. Li, E. Xie, Y. Liu, Z. Xie, J. Wang, C. Yu, W. Lan, *Sci. Adv.* **2023**, *9*, eadh8083.
[270] S. Lin, H. Maekawa, S. Moeinzadeh, E. Lui, H. V. Alizadeh, J. Li, S. Kim, M. Poland, B. C. Gadomski, J. T. Easley, J. Young, M. Gardner, D. Mohler, W. J. Maloney, Y. P. Yang, *Nat. Commun.* **2023**, *14*, 4455.

[271] S. O. Blacklow, J. Li, B. R. Freedman, M. Zeidi, C. Chen, D. J. Mooney, *Sci. Adv.* **2019**, *5*, eaaw3963.
[272] A. M. Nash, M. I. Jarvis, S. Aghlara-Fotovat, S. Mukherjee, A. Hernandez, A. D. Hecht, P. D. Rios, S. Ghani, I. Joshi, D. Isa, Y. Cui, S. Nouraein, J. Z. Lee, C. Xu, D. Y. Zhang, R. A. Sheth, W. Peng, J. Oberholzer, O. A. Igoshin, A. A. Jazaeri, O. Veiseh, *Sci. Adv.* **2022**, *8*, eabm1032.
[273] H. Qu, C. Gao, K. Liu, H. Fu, Z. Liu, P. H. J. Kouwer, Z. Han, C. Ruan, *Nat. Commun.* **2024**, *15*, 2930.
[274] J. Li, S. Sudiwala, L. Berthoin, S. Mohabbat, E. A. Gaylord, H. Sinada, N. C. Pacheco, J. C. Chang, O. Jeon, I. M. A. Lombaert, A. J. May, E. Alsberg, C. S. Bahney, S. M. Knox, *Sci. Adv.* **2022**, *8*, eadc8753.
[275] K. Mendez, W. Whyte, B. R. Freedman, Y. Fan, C. E. Varela, M. Singh, J. C. Cintron-Cruz, S. E. Rothenbücher, J. Li, D. J. Mooney, E. T. Roche, *Adv. Mater.* **2024**, *36*, 2303301.
[276] Y. Zhu, Z. Yang, Z. Pan, Y. Hao, C. Wang, Z. Dong, Q. Li, Y. Han, L. Tian, L. Feng, Z. Liu, *Sci. Adv.* **2022**, *8*, eabo5285.
[277] D. Wang, S. Maharjan, X. Kuang, Z. Wang, L. S. Mille, M. Tao, P. Yu, X. Cao, L. Lian, L. Lv, J. J. He, G. Tang, H. Yuk, C. K. Ozaki, X. Zhao, Y. S. Zhang, *Sci. Adv.* **2022**, *8*, eabq6900.
[278] R. Tan, X. Yang, H. Lu, Y. Shen, *Nat. Commun.* **2024**, *15*, 4761.
[279] G. Chen, F. Wang, M. Nie, H. Zhang, H. Zhang, Y. Zhao, *Proc. Natl. Acad. Sci. USA* **2021**, *118*, e2112704118.
[280] J. Zhu, Y. He, Y. Wang, L.-H. Cai, *Nat. Commun.* **2024**, *15*, 5902.
[281] J. A. Hubbell, *Biotechnology* **1995**, *13*, 565.
[282] W. Rajapaksha, I. H. W. Nicholas, T. Thoradeniya, D. N. Karunaratne, V. Karunaratne, *RSC Pharm.* **2024**, *1*, 259.
[283] A. Parvaresh, Z. Izadi, H. Nemati, H. Derakhshankhah, M. Jaymand, *J. Mol. Liq.* **2023**, *382*, 121990.
[284] S. Wu, J. Wu, H. Yu, J. Zhang, J. Huang, L. Zhou, L. Deng, H. Li, *Int. J. Biol. Macromol.* **2024**, *270*, 132387.
[285] W. Liao, X. Duan, F. Xie, D. Zheng, P. Yang, X. Wang, Z. Hu, *Int. J. Biol. Macromol.* **2023**, *236*, 123952.
[286] Z. Ferjaoui, R. López-Muñoz, S. Akbari, H. Issa, A. Semlali, F. Chandad, M. Rouabhia, D. Mantovani, R. Fanganiello, *Adv. Eng. Mat.* **2024**, *26*, 2400247.
[287] J. Wang, Y. Qi, Y. Gui, C. Wang, Y. Wu, J. Yao, J. Wang, *Small* **2024**, *20*, 2305951.
[288] W. Wang, D. Yao, H. Wang, Q. Ding, Y. Luo, H. Ding, J. Yu, H. Zhang, K. Tao, S. Zhang, F. Huo, J. Wu, *Adv. Funct. Mater.* **2024**, *34*, 2316339.
[289] G. Park, H. Park, J. Seo, J. C. Yang, M. Kim, B. J. Lee, S. Park, *Nat. Commun.* **2023**, *14*, 3049.
[290] M. Chen, J. Jiang, W. Guan, Z. Zhang, X. Zhang, W. Shi, L. Lin, K. Zhao, G. Yu, *Adv. Mater.* **2024**, *36*, 2311416.
[291] M. Fizir, S. Touil, A. Richa, L. Wei, S. Douadia, R. Taibi, S. Cherifi, D. S. Mansuroglu, P. Dramou, *Appl. Clay Sci.* **2024**, *256*, 107430.
[292] H. Peng, Y. Chen, J. Lin, C. Benally, M. G. El-Din, J. Gao, *Front. Environ. Sci. Eng.* **2024**, *18*, 51.
[293] N. Gao, Q. Zhang, Y. Fan, Z. Chen, Y. Zhang, J. Gao, J. Shi, H. Wang, K. Zhao, L. Lin, *Desalination* **2024**, *591*, 117984.
[294] N. Azizeh, A. Karam, A. Heer, M. Najlah, R. Singer, R. G. Alany, S. W. Gould, M. Khoder, *Carbohydr. Polym.* **2024**, *326*, 121604.
[295] W. Huang, Q. Ding, H. Wang, Z. Wu, Y. Luo, W. Shi, L. Yang, Y. Liang, C. Liu, J. Wu, *Nat. Commun.* **2023**, *14*, 5221.
[296] R. Tong, Z. Ma, P. Gu, R. Yao, T. Li, M. Zeng, F. Guo, L. Liu, J. Xu, *Int. J. Biol. Macromol.* **2023**, *246*, 125683.
[297] R. Zhang, C. Wu, W. Yang, C. Yao, Y. Jing, N. Yu, S. Su, S. Mahmud, X. Zhang, J. Zhu, *Ind. Crops Prod.* **2024**, *210*, 118187.
[298] X. Zou, P. Li, Z. Zhao, Y. Wu, D. Ma, Y. Song, J. Wang, *J. Electroanal. Chem.* **2023**, *941*, 117554.
[299] F. Benali, B. Boukoussa, I. Issam, A. Mokhtar, J. Iqbal, M. Hachemaoui, F. Habeche, Z. cherifi, S. Hacini, S. P. Patole, M. Abboud, *J. Polym. Environ.* **2023**, *31*, 4170.
[300] W. Zhong, Q. Peng, Y. Li, X. Tang, K. Liu, *Sep. Purif. Technol.* **2025**, *354*, 129238.
[301] G. Qin, X. Song, Q. Chen, W. He, J. Yang, Y. Li, Y. Zhang, J. Wang, D. D. Dionysiou, *Appl. Catal., B* **2024**, *344*, 123640.
[302] J. Zhu, Y. Wang, X. Zhao, N. Li, X. Guo, L. Zhao, Y. Yin, *Int. J. Biol. Macromol.* **2024**, *267*, 131450.
[303] J. Ma, B. Song, X. Li, T. Zhang, T. Liu, Y. Dang, G. Tian, *J. Text. Inst.* **2023**, *114*, 1070.
[304] X. Yue, W. Deng, Z. Zhou, Y. Xu, J. He, Z. Wang, *J. Polym. Environ.* **2023**, *31*, 1038.
[305] S. Wang, Y. Yang, C. Wang, Y. Jiao, C. Wang, H. Ma, *Cellulose* **2024**, *31*, 8787.
[306] J. Lv, Z. Li, R. Dong, Y. Xue, Y. Wang, Q. Li, *Int. J. Biol. Macromol.* **2023**, *247*, 125834.

Pietro Tordi obtained his Master's degree in Chemical Sciences from the University of Florence. He is currently pursuing a joint Ph.D. program at the Institut de Science et d'Ingénierie Supramoléculaires (University of Strasbourg) and the Department of Chemistry "Ugo Schiff" (University of Florence). His research focuses on the development of biopolymer-based functional materials for applications in sensing and energy storage.

Francesca Ridi is an associate professor in Physical Chemistry at the Department of Chemistry "Ugo Schiff," University of Florence, Italy, and member of CSGI Consortium. She is member of the board of the Division of Physical Chemistry of the Italian Chemical Society. She was PI or participant in several projects funded by EU, Italian Ministry or industrial collaborations. Her scientific interests are in the study of the physico-chemical properties of inorganic colloidal materials and their interaction with organic molecules, for applications spanning from building materials to biomedicine. She published 86 papers in international journals (H-index 31, more than 2300 citations).

Paolo Samorì is Distinguished Professor at the University of Strasbourg and Former Director of the Institut de Science et d'Ingénierie Supramoléculaires (ISIS). He is Member of the Académie des technologies, Member of ACATECH, Foreign Member of the Royal Flemish Academy of Belgium for Science and the Arts, Fellow of the Royal Society of Chemistry, Fellow of the European Academy of Sciences, Member of the Academia Europaea, Fellow of the Materials Research Society (MRS) and Senior Member of the Institut Universitaire de France. He published 480+ papers on two-dimensional materials and functional organic/polymeric nanomaterials for optoelectronics, energy storage and sensing.

Massimo Bonini is an associate professor of Physical Chemistry at the Department of Chemistry "Ugo Schiff," University of Florence. He earned his Chemistry degree in 1999 and his doctorate in 2004. His career includes roles as a Postdoctoral researcher in Florence, a Visiting Fellow at the Australian National University, and a Marie Curie Fellow at BASF SE and the Institute of Science and Engineering in Supramolecular Chemistry in Strasbourg. He has published over 85 articles (3900+ citations, h-index 34) and holds 3 patents. Since 2023, he is the President of the Materials Science Degree program at the University of Florence.